
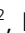













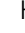




Status and Performance of the ShakeAlert Earthquake Early Warning System: 2019–2023

Angela I. Lux¹, Deborah Smith², Maren Böse³, Jeffrey J. McGuire², Jessie K. Saunders⁴, Minh Huynh², Igor Stubailo⁴, Jennifer Andrews^{4,5}, Gabriel Lotto⁶, Brendan Crowell⁶, Stephen Crane⁷, Richard M. Allen¹, Douglas Given², Renate Hartog⁶, Thomas Heaton⁴, Allen Husker⁴, Julien Marty¹, Leland O'Driscoll⁸, Harold Tobin⁶, Sara K. McBride², and Douglas Toomey⁸

ABSTRACT

The U.S. Geological Survey (USGS)-operated ShakeAlert® system is the United States West Coast earthquake early warning system (Given *et al.*, 2018). In this study we detail ShakeAlert's performance during some of the largest events seen by the system thus far. Statewide public alerting using ShakeAlert messages was authorized in California in October 2019. Over the next few years, public alerts were expanded into Oregon and then into Washington (U.S. Geological Survey, 2024). ShakeAlert source results are routinely compared to the USGS Comprehensive Catalog (ComCat; Guy *et al.*, 2015; U.S. Geological Survey, Earthquake Hazards Program, 2024), which contains the earthquake location and magnitude determined using complete waveform data. M 4.5 and larger is the threshold used for public alerting and was deliberately set below the level where damage is likely to compensate for cases where the system underestimates the magnitude. Between 17 October 2019 and 1 September 2023, the ShakeAlert system created 95 events with maximum magnitude estimates of $M \geq 4.5$, the public alerting threshold. 94 of the 95 events were due to real earthquakes. Seven were categorized "false" per ShakeAlert's internal definition that there was no matching catalog event within 100 km and 30 s of origin time; however, all but one of these were real earthquakes that were poorly located, primarily because they were at the edges of the seismic network. Three detected events were labeled "missed" because they were very poorly located (> 100 km location error). In addition, the system did not produce solutions for four ComCat events $M \geq 4.5$ (U.S. Geological Survey, Earthquake Hazards Program, 2024), which were all at the edge of the alerting and network boundaries. The ShakeAlert system has accurately detected the majority of earthquakes that have occurred within the operational region since completing the public rollout, and alerts from the system have been delivered to millions of cell phone users throughout the West Coast.

KEY POINTS





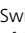







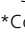

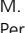

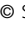

- We seek to understand the performance of ShakeAlert, the United States West Coast earthquake early warning (EEW) system since public alerting began.
- ShakeAlert has created accurate and timely alerts for many earthquakes since October 2019.
- We anticipate that ShakeAlert will continue to provide useful alerts for future West Coast earthquakes.

Supplemental Material

INTRODUCTION

ShakeAlert introduction

ShakeAlert is a public earthquake early warning (EEW) system being developed and operated for the United States (US) West Coast by researchers, developers, and network operators at University of California Berkeley, the California Institute of

1. UC Berkeley Seismological Laboratory (UCB), Berkeley, California, U.S.A.,  <https://orcid.org/0000-0002-3767-6018> (AIL);  <https://orcid.org/0000-0003-4293-9772> (RMA); 2. U.S. Geological Survey (USGS), Pasadena, California, U.S.A.,  <https://orcid.org/0000-0001-9235-2166> (JJMG);  <https://orcid.org/0000-0002-5856-121X> (MH);  <https://orcid.org/0000-0002-3277-5121> (DG);  <https://orcid.org/0000-0002-8062-6542> (SKMB); 3. Swiss Seismological Service (SED), ETH Zürich, Switzerland,  <https://orcid.org/0000-0003-4639-719X> (MB); 4. California Institute of Technology (Caltech) Seismological Laboratory, Pasadena, California, U.S.A.,  <https://orcid.org/0000-0001-5340-6715> (JKS);  <https://orcid.org/0000-0001-7657-2783> (IS);  <https://orcid.org/0000-0002-5679-5565> (JA);  <https://orcid.org/0000-0003-3363-2197> (TH);  <https://orcid.org/0000-0003-1139-0502> (AH); 5. GNS Science, Lower Hutt, New Zealand; 6. Department of Earth and Space Sciences, University of Washington (UW), Seattle, Washington, U.S.A.,  <https://orcid.org/0000-0002-0595-2305> (GL);  <https://orcid.org/0000-0001-7096-601X> (BC);  <https://orcid.org/0000-0002-4116-7806> (RH);  <https://orcid.org/0000-0002-1447-6873> (HT); 7. Natural Resources Canada (NRCAN), Ottawa, Canada,  <https://orcid.org/0000-0003-2365-9361> (SC); 8. University of Oregon (UO), Eugene, Oregon, U.S.A.,  <https://orcid.org/0000-0003-2873-4084> (DT)

*Corresponding author: angie.lux@berkeley.edu

Cite this article as Lux, A. I., D. Smith, M. Böse, J. J. McGuire, J. K. Saunders, M. Huynh, I. Stubailo, J. Andrews, G. Lotto, B. Crowell, *et al.* (2024). Status and Performance of the ShakeAlert Earthquake Early Warning System: 2019–2023, *Bull. Seismol. Soc. Am.* **XX**, 1–22, doi: [10.1785/0120230259](https://doi.org/10.1785/0120230259)

© Seismological Society of America

Technology, Eidgenössische Technische Hochschule Zürich, University of Oregon, University of Washington, University of Nevada, Reno, Central Washington University, the Geodetic Facility for the Advancement of Geosciences, and the U.S. Geological Survey (USGS; [Given et al., 2018](#)). The USGS publishes earthquake information provided by ShakeAlert and alerts are then issued by official alert delivery partners ([Given et al., 2018](#)).

The original ShakeAlert project began in 2007 as the California Integrated Seismic Network ShakeAlert system ([Böse et al., 2014](#)), and included the ElarmS ([Allen and Kanamori, 2003](#); [Allen, 2007](#); [Allen et al., 2009](#)), Onsite ([Kanamori, 2005](#); [Wu et al., 2007](#); [Böse, Hauksson, Solanki, Kanamori, and Heaton, 2009](#); [Böse, Hauksson, Solanki, Kanamori, et al., 2009](#)), and virtual seismologist (VS; [Cua and Heaton, 2007](#); [Cua et al., 2009](#)) algorithms. Over time this system has evolved. VS was retired in 2016, and in 2018 the ElarmS point-source algorithm was updated to include a modified waveform filter from the Onsite algorithm and rebranded as the Earthquake Point-source Integrated Code (EPIC; [Brown et al., 2011](#); [Kuyuk et al., 2014](#); [Chung et al., 2019](#)). As EPIC is a point-source algorithm with a magnitude estimate that saturates around $M \sim 6.5$ to 7, the Finite-fault rupture Detector (FinDer; [Böse et al., 2012, 2015, 2018](#), [Böse, Andrews, Hartog, and Felizardo, 2023](#)) algorithm was added to ShakeAlert in March 2018 to address the need to accurately characterize larger earthquakes, including a finite-source description.

The ShakeAlert system has been rolled out throughout the US West Coast in phases to ensure maximum reliability and public confidence in the system ([Kohler et al., 2018, 2020](#)). To successfully deliver alerts to the public in California, Oregon, and Washington, the network of seismic stations used by the system in each state must be dense enough for the system to rapidly detect all significant earthquakes in that area. This article covers the performance of ShakeAlert from 2019 to 2023—a period when the contributing seismic networks were rapidly expanding their station coverage to meet ShakeAlert’s design goals and the production system, including the EEW algorithms, was being continually adapted to improve performance.

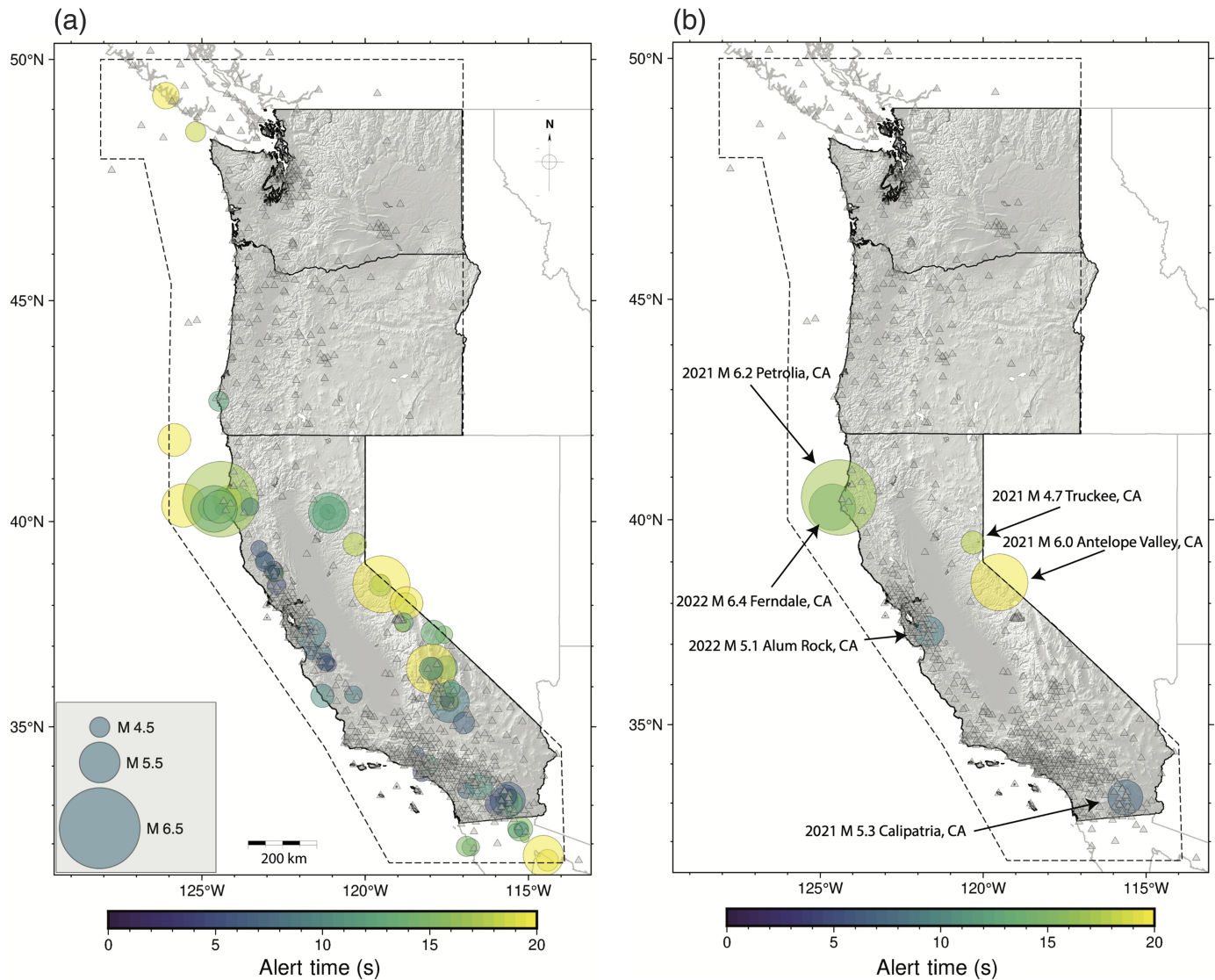
In October 2018, the ShakeAlert system “opened for business” ([Kohler et al., 2020](#)) for limited applications by pilot users but not for large-scale public alerting. The first large-scale test of public alerting began in December 2018 in Los Angeles County using a cell phone app developed by the City of Los Angeles ([Lin, 2019](#)). Because of the sensitive nature of generating emergency alerts for the public, the USGS established agreements with emergency management officials within each state before the general public could receive alerts there. Alerting thresholds were determined jointly with the state emergency management agencies: the California Office of Emergency Services, the Washington Emergency Management Division, and the Oregon Department of Emergency Management. ShakeAlert began publishing live alerts for pilot partners throughout

California on 29 September 2019, and 17 October 2019 alerts for the general public became available state-wide through the MyShake ([Allen et al., 2019](#); [Patel and Allen, 2022](#)) and QuakeAlertUSA (refer to [Data and Resources](#)) cell phone apps and through the wireless emergency alert (WEA) system operated by the Federal Emergency Management Agency (FEMA; [McBride et al., 2023](#)). Public alerting began in Oregon and Washington in March 2021 and May 2021, respectively. QuakeAlertUSA distributed alerts until it was retired in November 2023.

ShakeAlert seismic network

The ShakeAlert system has evolved significantly because limited test notifications to pilot developers in California began in January 2012. Its continued expansion and development have depended on the simultaneous expansion of the United States seismic networks stretching between the borders of Mexico and Canada. In 2012, the ShakeAlert seismic network consisted of approximately 700 seismic stations. ShakeAlert now ingests data from 1509 broadband and strong-motion stations in the Advanced National Seismic System West Coast networks and California State networks combined (as of December 2023). The final station count in the ShakeAlert Technical Implementation Plan ([Given et al., 2018](#)) is 1675 stations, which may be achieved by 2025. To optimize detection and alerting in seismically active areas with high population, such as the San Francisco Bay Area and Los Angeles, the plan calls for a station spacing of 10 km. Outside of these urban areas, ShakeAlert is striving for an average station spacing of 20 km in seismic source areas that endanger population centers and 40 km in areas with lower seismic risk ([Given et al., 2018](#)).

Regions of sparse station coverage can be a challenge for ShakeAlert. EPIC requires P wave triggers from at least 40% of stations within the radius of the farthest trigger associated with that event to create an alert (with a minimum of four triggering stations). Because of its highly sensitive triggering algorithm, EPIC frequently triggers undesired signals including very small local earthquakes, anthropogenic noise, station recalibrations, and spurious signals. Although many of those triggers are filtered out by the algorithm ([Chung et al., 2019](#)), some still pass through. Such triggers in a sparsely instrumented region can generate a false or incorrect alert, for example, when EPIC associates three triggers from a very small earthquake with one more distant spurious trigger. Though unlikely, it has happened that because of sparse station coverage in an area, the association of such triggers results in the estimated location of the small earthquake being pushed far from the true epicenter (because there are no nearby stations to constrain the location estimate) and the magnitude increased dramatically to correspond with the poor location. FinDer’s event detection in ShakeAlert was originally configured as four neighboring (within 50 km) stations detecting seismic ground motions above 2 cm/s/s. This threshold was



chosen conservatively to minimize false alerts; however, it comes at the expense of speed. Since 2018, FinDer has produced only two false alerts with estimated magnitudes equal to or above 4.0 (M 4.0 and 4.4), both related to earthquakes in northern California but with large errors in location (~ 125 km) and origin time (~ 35 s) due to contamination by signals from a malfunctioning sensor (Böse, Andrews, Hartog, and Felizardo, 2023). The latest version of FinDer (v.3; Böse, Andrews, Hartog, and Felizardo, 2023) uses a dynamic trigger radius when spatially associating triggers, which computes a per-station radius at the time of event detection according to that station's amplitude, taking into account only the stations that actively contribute data.

Ensuring an adequate density of stations is thus critically important for not only ensuring timely alerts, but also for preventing false and problematic alerts, and so continues to be a high priority for the ShakeAlert system. Edge-of-network earthquakes (see Fig. 1 for the ShakeAlert reporting boundary), such as those offshore, in Mexico, Nevada, and so on, can also create problems for the ShakeAlert system. The lack of

Figure 1. (a) Map showing epicentral locations of all earthquakes with ShakeAlert magnitude estimates $M \geq 4.5$ within the ShakeAlert alerting boundary (Given *et al.*, 2018) (dashed line) from 17 October 2019 to 1 September 2023 (87 events; U.S. Geological Survey, Earthquake Hazards Program, 2024). Earthquakes (circles) colored by alert time (time between earthquake origin time and when ShakeAlert published an alert message), with sizes showing relative Comprehensive Catalog (ComCat; U.S. Geological Survey, Earthquake Hazards Program, 2024) magnitude. Triangles are seismic stations used by the ShakeAlert system as of 1 September 2023. (b) Same as panel (a), but only showing earthquakes discussed in detail in this article: 2021 M 4.7 Truckee, California; 2021 M 5.3 Calipatria, California; 2021 M 6.0 Antelope Valley, California; 2021 M 6.2 Petrolia, California; 2022 M 5.1 Alum Rock, California; and 2022 M 6.4 Ferndale, California. The color version of this figure is available only in the electronic edition.

sufficient azimuthal station coverage makes locating and characterizing an earthquake challenging for the system, as was seen in the 2021 M 6.0 Antelope Valley and 2021 M 6.2 Petrolia earthquakes, which we will discuss in detail subsequently. During offshore and out-of-network events, poor azimuthal coverage can cause EPIC to push its epicenter

estimate farther outside the network and increase magnitude estimates (Williamson *et al.*, 2023). FinDer tends to have the opposite behavior given poor azimuthal coverage: its location estimates during these events tend to be closer to or within the network and magnitude estimates decrease (Böse, Andrews, *et al.*, 2023). Incorporation of stations from the Nevada, United States, Canada, and Baja California, Mexico (Red Sísmica del Noroeste de México) seismic networks has dramatically improved the performance of ShakeAlert in these edge-of-network and out-of-network events.

In addition to increasing the number of stations that contribute to ShakeAlert, improvements have been made in how station data get delivered to the ShakeAlert processing centers. For example, after unexpectedly slow data delivery was observed during the 2019 *M* 7.1 Ridgecrest, California, earthquake (Stubailo *et al.*, 2020), the Southern California Seismic Network (SCSN; California Institute of Technology and United States Geological Survey Pasadena, 1926) made progress in upgrading telemetry links and reconfigured data delivery routes around that area. All radios at CLXGPO (a major telemetry hub, 35.65° N, 117.67° W; SCEDC, refer to Data and Resources) have been upgraded to modern Cambium N550 900 Mhz units and linked together with multiple master synchronization to better coordinate sending and receiving of all radio links. This reduces interference and improves the timeliness of data delivery. The CLXLRL (35.48° N, 117.68° W)-CLXGPO connection has also been upgraded with a high throughput Cambium 4.4 GHz radio to support a large volume of data from multiple sites.

To verify the network improvements and to compare telemetry connections before and after the upgrades, SCSN developed tools to measure the performance. Telemetry recovery test (TRT) simulates the increased data volume that would be generated during large events due to lower data compressibility (Stubailo *et al.*, 2023). The volume variability is explained by the STEIM2 compression algorithm design used by the SCSN seismic dataloggers (Steim and Spassov, 2017). While compressing, the STEIM2 algorithm removes as many redundant data points (similar bits) as possible, but during a strong seismic event, when the data becomes very heterogeneous and with larger amplitude ground motions, that compression rate drops almost to zero (Steim and Spassov, 2017). TRT stops the seismic data flow on the data center side and resumes it after 15 min for three sites at a time for SCSN. The idea of the method is to find a point in time when the latency of the gradually delivered buffered data becomes equal to the pretest mean values (Stubailo *et al.*, 2020). The time-to-deliver buffered by the dataloggers data correlates with the throughput of the telemetry connection between a seismic site and the data center, and long delivery times can be used to identify struggling links.

TRT results confirmed the low-performing connections during the Ridgecrest sequence. The transport real-time data

latency alone outside of the TRT cannot measure the link throughput; it only measures the packet travel time. To measure a link capacity, one would need to perform a stress test by maximizing the data volume and measuring how much data is successfully transferred from the source (logger) to the destination (data center) and at what speed. This technique is similar to the one described in Antoniadou *et al.* (2006) and Jain and Dovrolis (2003), but with application to the seismic data flow.

Public alerting rollout

The first phase of the ShakeAlert system's rollout occurred in the fall 2018 when more than 60 institutional partners began receiving EEW alerts from the system (Kohler *et al.*, 2020). With this rollout, approved technical partners could use ShakeAlert information beyond proof-of-concept projects, including taking their products to market. ShakeAlert publishes alert information for events with estimated magnitudes of *M* ≥ 3.5 ; however, *M* 4.5 is the threshold for public alerting. Alert products include event source messages containing the estimated hypocenter location, origin time, line source (*M* ≥ 6 earthquakes), and magnitude of the earthquake; contour messages with ground-motion estimates represented as nested contours for each modified Mercalli intensity (MMI) level greater than 2; and map messages that describe the ground-motion estimates as a grid of points with expected MMI, peak ground acceleration (PGA), and peak ground velocity (PGV) values (Given *et al.*, 2018). Technical partners then use this information to deliver alerts to users. Technical partners are held to technical performance standards, which require them to “make all reasonable efforts to maintain a median time to receive, process, and redistribute the alerts from the ShakeAlert system to its clients of no more than five (5) seconds.” (ShakeAlert website, see Data and Resources). In addition, automated actions initiated by users must be tolerant of false, missed, and late alerts (Kohler *et al.*, 2020).

On 17 October 2019, statewide alerts became directly available to the public in California, marking an important milestone in the ShakeAlert project (Bostrom *et al.*, 2022). Cell phone alert delivery options included WEA and three cell phone apps operated by ShakeAlert licensed to operate partners—MyShake, operated by the University of California at Berkeley (Patel and Allen, 2022); QuakeAlertUSA, operated by EarlyWarningLabs (now retired, Woolfolk, 2023) (QuakeAlertUSA website, refer to Data and Resources); and ShakeAlertLA, operated by the City of Los Angeles (now retired; ABC7 News, refer to Data and Resources). At that time both MyShake and QuakeAlertUSA alerted anyone with the app within the California alerting boundary; ShakeAlertLA specifically warned users located within the limits of the County of Los Angeles (Ruan *et al.*, 2022). In August 2020, ShakeAlert licensed-to-operate partner Google incorporated an alerting capability into its Android operating system, allowing Android mobile users the capability to receive alerts

of impending shaking based on ShakeAlert messages (Allen and Stogaitis, 2022). Most recently, the ShakeReadySD app was released by ShakeAlert licensed to operate partner San Diego County in 2022 (refer to Data and Resources).

All methods of cell phone alerts have both magnitude and intensity alerting thresholds. WEA alerts are distributed to users within cell phone tower regions for estimated magnitude ≥ 5.0 and for which shaking intensity is expected to be $\text{MMI} \geq 4$ (McBride *et al.*, 2023). As with other published studies, here we follow the convention of Wald *et al.* (1999) that an integer MMI value refers to instrumental intensities within 0.5 of that value (e.g., MMI 4 intensity category includes the range MMI 3.5–4.5). The ShakeAlert contour product specifically computes polygons corresponding to the lower extent of a given MMI category (i.e., the MMI 4 contour is the estimated extent of MMI 3.5; Chung *et al.*, 2020). As WEA alerts are issued via the FEMA's Integrated Public Alert and Warning System (FEMA, 2023), they are restricted to criteria that meet a statutory requirement of "imminent threat" and hence utilize a higher alerting threshold than some other alert delivery mechanisms (McBride *et al.*, 2023). Many cell phone apps have lower thresholds, alerting for earthquakes with estimated magnitudes of $M \geq 4.5$, and to users where shaking intensity is estimated to be MMI 3 and above.

The public alerting rollout continued northward to include Oregon and Washington in March 2021 and May 2021, respectively (Sumy, Jenkins, *et al.*, 2022). Android cell phone users in Oregon and Washington may be alerted by their phones' operating system or by the MyShake app (Sumy, Jenkins, *et al.*, 2022). QuakeAlertUSA was operational in Oregon until November 2023 (Woolfolk, 2023).

ShakeAlert communication, education, outreach, and technical engagement

The ShakeAlert system is supported by a robust outreach and engagement apparatus, known as the Joint Committee for Communication, Education, Outreach, and Technical Engagement (JCCEO&TE; de Groot *et al.*, 2022). The long-standing priorities of ShakeAlert JCCEO&TE are public safety, preparedness, and resilience; technical implementation and engagement; consistent messaging and communication; integration with other federal and state earthquake hazards products; and educational resource development and dissemination (de Groot *et al.*, 2022). ShakeAlert JCCEO&TE is made up of three permanent working groups: the Education Resources Working Group (ERWG), the Social Science Working Group (SSWG), and the Technical Users Working Group (TUWG).

The ERWG is responsible for developing educational resources about the ShakeAlert system and earthquake safety, with a special focus on resources for school and free-choice learning (e.g., libraries and museums) settings (Sumy, Jenkins, McBride, and de Groot, 2022). Educational resources are also developed for emergency managers as well as ShakeAlert

technical partners and end users. Resources include classroom activities and demonstrations, videos, graphics, and fact sheets (refer to Data and Resources). The ERWG is composed of an interdisciplinary group of educators, geoscientists, and other stakeholders who aim to communicate clearly with a wide variety of audiences.

The SSWG conducts and coordinates social science research related to ShakeAlert and EEW (Goltz, 2023; McBride and DeGroot, 2023). Research topics include human response to alerting, knowledge about EEW and earthquake preparedness, earthquake protective actions, and issues related to diversity, equity, inclusion, and accessibility (DEIA; McBride and DeGroot, 2023). SSWG members include USGS social scientists and a broad community of social science researchers from across the globe. The SSWG's research findings contribute directly to operational decisions relating to the ShakeAlert system's public messaging (Bostrom *et al.*, 2022; Crayne *et al.*, 2023), alerting priorities and limitations (McBride *et al.*, 2023), post-alert messaging (McBride *et al.*, 2020; Sutton *et al.*, 2023), and ensuring that communication and education of ShakeAlert considers diversity and inclusion (Jenkins *et al.*, 2022). Further, SSWG research has informed advice regarding ShakeAlert and personal protective actions (McBride *et al.*, 2022), demographics of knowledge about EEW (Adams *et al.*, 2022), and access to information via museums and free choice learning environments (Sumy, Jenkins, McBride, and de Groot, 2022; Sumy *et al.*, 2023), and more (McBride and DeGroot, 2023). Overall, SSWG members have produced more than 40 articles, book chapters, conference papers, and government reports since its inception in 2019, arguably not only increasing knowledge about what publics know and understands about EEW systems, but also earthquakes in general on the West Coast of the United States (McBride and DeGroot, 2023).

The mission of the TUWG is to recruit, engage, and support ShakeAlert technical partners (any entity that enters into a license agreement with the USGS to use USGS-issued ShakeAlert messages for alerting applications (de Groot *et al.*, 2022), leading to the broad, diverse, and sustainable implementation of ShakeAlert-powered products and services. TUWG membership is composed of Technical Engagement Regional Coordinators, working at the USGS and partnering universities. A larger group of TUWG collaborators includes representatives from state emergency management agencies and geological surveys. The TUWG assists prospective technical partners in developing ShakeAlert-powered implementations and navigating the USGS licensing pathway. Organizations become technical partners by signing a pilot license agreement with the USGS. After demonstrating that their pilot project fulfills the technical as well as the education and outreach requirements established by the USGS, pilot partners are granted a license to operate (LtO). LtO partners may continue to use ShakeAlert data for their purposes (e.g., alerting employees through desktop computers or automatically slowing trains) or may choose to distribute a product

broadly to end-users, for example, building a cell phone app for the public, or selling hardware products that interact with water utility control systems and throttle water valves). By the end of 2023, there were 13 technical partners with LtO status (System Information, LtO Technical Partners section of the ShakeAlert website; refer to [Data and Resources](#)), and an additional 14 technical partners working on one or more pilot projects. The total number of end-user organizations—those who have purchased a ShakeAlert-powered product or service from an LtO partner—is unknown to the USGS ShakeAlert team.

ShakeAlert system

The ShakeAlert system ([Given *et al.*, 2018](#)) includes the EPIC and FinDer EEW algorithms as well as the solution aggregator (SA), decision module (DM), and eqinfo2GM modules ([Thakoor *et al.*, 2019](#)). The first step of ShakeAlert processing is the data layer ([Given *et al.*, 2018](#)). Here, raw data from sensors throughout the West Coast are continuously sent to data-processing centers in Seattle, Washington; Menlo Park, California; Pasadena, California; and Berkeley, California (refer to [Data and Resources](#)). Dedicated waveform processing modules for each of the EEW algorithms process the incoming data and extract the necessary ground-motion metrics (e.g., PGA) required by each algorithm. These processed data enter the Production layer and are fed into the EPIC and FinDer seismic EEW algorithms. While EPIC can quickly detect earthquakes, it is a point-source algorithm and is limited to only using the initial ~ 4 s of the *P*-wave arrival, which results in a saturation of the magnitude estimate at $M \sim 6.5$ to 7. FinDer, by contrast, is a finite-source algorithm and characterizes the earthquake as a fault rupture along a line source or as a new development along more complex sources ([Böse, Andrews, Hartog, and Felizardo, 2023](#)). FinDer estimates are typically a bit slower than those from EPIC due to a conservatively chosen trigger criterion as well as due to requiring observations of high (≥ 2 cm/s) PGAs rather than *P*-wave observations. However, since FinDer is sensitive to spatial ground-motion distributions rather than absolute ground-motion amplitudes, it can estimate the magnitude of an earthquake as large as M 9 in addition to smaller earthquakes with magnitudes $M \leq 3$ ([Böse *et al.*, 2018](#)). It should be emphasized that FinDer is designed to characterize spatial ground-motion distributions (as required for EEW), not to provide accurate source descriptions. For events that radiate unusually strong high-frequency motions (e.g., high-stress drop events), FinDer will adjust its magnitude and possibly location estimates to reduce ground motion residuals. Additional information and detailed performance analysis for FinDer from March 2018 to October 2022 can be found in [Böse, Andrews, Hartog, and Felizardo \(2023\)](#).

The point-source solution from EPIC, containing an estimated location and magnitude, and the finite-source solution from FinDer, with an estimated line-source location, orientation (strike), and a length of fault rupture as well as an

estimated ground-motion centroid location and magnitude, are then combined into a single unified solution by the SA ([Given *et al.*, 2018](#)). If both algorithms provide solutions, and they are associated in space and time by the stations used by each algorithm to create the detections, then the location and magnitude estimations from both EPIC and FinDer are combined and assigned weights based on their corresponding error estimates. If the FinDer magnitude estimate exceeds M 6 and is also above the EPIC magnitude estimate, the SA will switch to using only FinDer's magnitude. If both EPIC and FinDer create magnitude estimates above M 6 and the EPIC magnitude is larger than the FinDer estimate, the two continue to be averaged together based on their corresponding magnitude uncertainty estimates. Until September 2022, it was necessary to obtain validation from EPIC before incorporating a FinDer report into a public alert. However, now FinDer can alert alone if it estimates the magnitude to be M 5.5 or larger (EPIC continues to be able to alert alone for all magnitudes). This strategy was modified after the 2021 M 6.0 Antelope Valley and 2021 M 6.2 Petrolia earthquakes (see below).

The SA checks whether the combined earthquake solution has a magnitude above the M 3.5 threshold and if it is within the ShakeAlert reporting boundary (Fig. 1) before passing the solution on to the ground-motion estimation module eqinfo2GM ([Thakoor *et al.*, 2019](#)). The eqinfo2GM module takes the unified solution with the earthquake location, magnitude, and fault rupture (if the combined magnitude is $M \geq 6$ and a line source is available from FinDer; if $M < 6$, only the point-source approximations are used), and applies ground-motion models (ground-motion prediction equation products, [Boore and Atkinson, 2008](#); [Chiou and Youngs, 2008](#); [Atkinson and Boore, 2011](#) and ground-motion-to-intensity conversion equations, [Worden *et al.*, 2012](#)) to create two products of estimated ground motion: a contour product and a map. The contour product creates eight-sided polygons of the estimated extent of ground motion above each MMI threshold. The map product estimates MMI on a grid with $0.2^\circ \times 0.2^\circ$ spacing, considering the site conditions models and data (time-averaged shear-wave velocity to 30 m depth V_{S30}) at each grid point rather than an average site condition used for the contour product (V_{S30} of 500 m/s). Both the contour and map products are currently defined as median shaking estimates ([Given *et al.*, 2018](#); [Thakoor *et al.*, 2019](#)). Although the map product is expected to be a more accurate estimate, the contour product is currently utilized by most ShakeAlert LtOs due to its small data packet with just eight data points needed to characterize the predicted ground motion at each MMI level.

The last step in the ShakeAlert system is the alert layer for which alerts are published to alerting channels following a final check by the DM ([Given *et al.*, 2018](#)) to ensure that the alert is within the alerting boundaries and has a magnitude larger than M 4.5. Once an alert is published, ShakeAlert LtOs can use the alert to notify end users. As more data come into the system

and the EPIC and FinDer solutions are updated, ShakeAlert continues to publish updated alerts with revised alerting polygons (Given *et al.*, 2018). Alert updates are allowed to be published as quickly as every 0.5 s if the combined source estimate changes meet one of the following threshold criteria: a magnitude change of at least 0.1 magnitude units; an epicenter change of at least 0.05°; an origin time change of at least 1 s; or other changes in the uncertainty estimates.

In addition to the production system, duplicate ShakeAlert systems are running on development, test, and integration machines, with code managed and version-controlled through a GitLab repository workflow (Given *et al.*, 2018). The development and test machines provide an environment in which algorithm updates and bug fixes can be prototyped and tested while running in real-time (Given *et al.*, 2018). If modifications to the code seem promising, the operation-ready code is then run on integration servers at each alert center, which are identical to the real-time production systems. After running on the integration servers, codes are then submitted to the ShakeAlert testing and certification group (Cochran *et al.*, 2018), which performs a series of replays and analyses to determine if and how the modified code improves the ShakeAlert system. Their analyses are then used to determine whether the new code will be implemented on the production machines.

SYSTEM PERFORMANCE

Matched, missed, and false events

ShakeAlert has published numerous EEW messages since statewide public alerting began in 2019 (Table 1). The performance of the system can be assessed in several ways, including whether ShakeAlert detected an earthquake, the alert accuracy (magnitude, location, and ground-motion estimates), and the timeliness of the alert. During the period between 17 October 2019 and 1 September 2023, the ShakeAlert system created 95 event detections with maximum magnitude estimates above the M 4.5 alerting threshold (refer to supplemental material available in this article). 94 of the 95 events were due to real earthquakes. 42 detections were overestimated and had USGS Comprehensive Catalog (ComCat; U.S. Geological Survey, Earthquake Hazards Program, 2024) magnitudes of $3.1 \leq M \leq 4.5$. ShakeAlert detected 46 of the 53 $M \geq 4.5$ earthquakes that occurred throughout the West Coast reporting region during this time and successfully published alert messages for 41 of those 46 detections (five of the ShakeAlert event estimates had peak magnitude estimates below the M 4.5 alert distribution threshold that were overestimated for a variety of reasons, including mislocations, site amplifications, and incorporation of S waves). The seven missed events during this time were all located at the edge of the network (five offshore northern California, one at the California–Nevada border, and one at the edge of the alerting boundary in Baja, Mexico). Of those seven missed events, three were detected by ShakeAlert but with poor location estimates due to poor azimuthal coverage

TABLE 1

Numbers of Matched, Missed, and False Alerts Created by the ShakeAlert System during the Time Period from 17 October 2019 to 1 September 2023 (U.S. Geological Survey, Earthquake Hazards Program, 2024)

Category	Number of Events
ShakeAlert detections with maximum magnitude $M \geq 4.5$	95
$M \geq 4.5$ ShakeAlert detections matching ComCat earthquakes (any distance)	94
$M \geq 4.5$ ShakeAlert detections matching ComCat magnitudes $M < 4.5$	42
ComCat $M \geq 4.5$ earthquakes	53
ComCat $M \geq 4.5$ earthquakes detected by ShakeAlert	46
ComCat $M \geq 4.5$ earthquakes with $M \geq 4.5$ ShakeAlert magnitude estimates	41
ComCat $M \geq 4.5$ earthquakes missed by ShakeAlert	7
$M \geq 4.5$ ShakeAlert detections with no ComCat earthquake within 100 km and 30 s of origin time (“false”)	7
$M \geq 4.5$ ShakeAlert detections with no corresponding ComCat earthquake	1

ComCat, Comprehensive Catalog.

(epicentral location estimate errors > 100 km). During this time, ShakeAlert created seven event estimates labeled “false” per ShakeAlert’s internal definition that there was no matching catalog event within 100 km and 30 s of the estimated origin time (Cochran *et al.*, 2018); however, all but one of these were real earthquakes that were poorly located, primarily because they were at the edges of the network.

As expected from the seismicity in this region, most of the detections occurred within and offshore California. During this time, there was one $M \geq 4.5$ earthquake in Oregon (30 November 2019 M 4.5 near Port Orford, Oregon). This coastal earthquake at the edge of the network was detected by ShakeAlert with both initial and final magnitude estimates of M 4.6 and a location error of 2.6 km at 12.3 s after origin time. No public alert was distributed during this event as public alerting was not available in Oregon at that time.

The three other earthquakes with $M \geq 4.5$ in the Pacific Northwest during this time were detected by ShakeAlert: an M 4.5 earthquake on 24 January 2020 (ShakeAlert initial estimate: M 4.5, 5.8 km location error, alert time 18.3 s; final estimate: M 4.2, 19 km location error), an M 4.8 earthquake on 10 May 2020 (ShakeAlert initial and final estimates: M 4.4 with 47 km location error, alert time 26.6 s), and an M 4.9 earthquake on 25 November 2022 (ShakeAlert initial estimate: M 5.2, 29 km location error, alert time 24.1 s; final estimate: M 4.8, 21 km location error). All three earthquakes were located offshore Vancouver Island in a region of sparse ShakeAlert station coverage, and none of them generated a public alert. Public alerting was not available during the earthquakes in 2020, and the MMI polygons for the M 4.8 earthquake in 2022 did not overlap the ShakeAlert alerting

boundary. The Pacific Northwest region will have denser station coverage with the integration of the Canadian EEW network into the ShakeAlert network as part of the Canadian EEW Program (Crane *et al.*, 2023). An offline real-time system test with the Canadian EEW network stations produced a better source estimate for the 25 November 2022 *M* 4.9 earthquake (offline ShakeAlert initial estimate: *M* 4.5, 2 km location error, 14.1 alert time).

Seventeen of the 53 ComCat (U.S. Geological Survey, Earthquake Hazards Program, 2024) *M* ≥ 4.5 earthquakes during this period occurred in the Mendocino Triple Junction region offshore Northern California (Fig. 1). The Mendocino Triple Junction is a particularly challenging area for the ShakeAlert system. Though additional stations have been added during the period covered in this study, there is still poor azimuthal coverage due to the geography of the region. The land directly to the east of the fracture zone protrudes to the west in such a way that azimuthal coverage in the initial alerts is often decreased further than if the coastline were a straight line. EPIC has difficulty constraining the location estimate with such poor azimuthal coverage, often pushing the location estimates far to the west. In contrast, FinDer typically shifts the estimated location to the east within the seismic network and reduces its magnitude estimate accordingly to match the observed ground motions.

Improving performance in the Mendocino Triple Junction has been a focus for both algorithms. FinDer now supports the capability to use fault-specific (including offshore) templates in addition to the generic line-source templates used before, and that capability may soon become part of the operational system (Böse, Andrews, Hartog, and Felizardo, 2023). A new version of EPIC currently under development includes a Bayesian approach that incorporates prior seismicity in its location estimation procedure (Williamson *et al.*, 2023). Offline testing has shown that this approach may improve location accuracy in regions of poor azimuthal coverage, including offshore and out-of-network areas.

The remaining earthquakes that ShakeAlert detected during the period from 17 October 2019 to 1 September 2023 were dispersed throughout California and included notable events in California, such as the 2021 *M* 4.7 Truckee earthquake, the 2021 *M* 5.3 earthquake near the Salton Sea, the 2021 *M* 6.0 Antelope Valley earthquake, the 2021 *M* 6.2 Petrolia earthquake, the 2022 *M* 5.1 Alum Rock earthquake, and the 2022 *M* 6.4 Ferndale earthquake. The performance of ShakeAlert during these events will be detailed in the following section.

Detailed performance analysis

The following section describes ShakeAlert performance during some of the more notable events that occurred between 17 October 2019 and 1 September 2023 while ShakeAlert was issuing public alerts, including the 2021 *M* 4.7 Truckee earthquake, the 2021 *M* 5.3 Calipatria earthquake, the 2021

M 6.0 Antelope Valley earthquake, the 2021 *M* 6.2 Petrolia earthquake, the 2022 *M* 5.1 Alum Rock earthquake, and the 2022 *M* 6.4 Ferndale earthquake (Fig. 1). Refer to Figures S2 and S3 for additional figures showing comparisons of observed PGA and PGV to ground-motion models used by ShakeAlert (Thakoor *et al.*, 2019) as well as ShakeAlert alert contours associated with the maximum magnitude alert for each event described subsequently.

2021 *M* 4.7 Truckee earthquake

The 7 May 2021 *M* 4.7 Truckee, California, earthquake (ComCat ID: nc73559265; U.S. Geological Survey, Earthquake Hazards Program, 2024) was an important event for ShakeAlert because it brought to light several issues with the system. ShakeAlert initially significantly overestimated the magnitude of this earthquake as *M* 6.0 with a location error of 29 km at 17.8 s after origin time. EPIC alone contributed to this estimate, and it continued to be the only algorithm to alert during this event. The first alert update from EPIC revised the magnitude estimate of *M* 3.8, with a final estimate of *M* 3.7. The first update published by the DM 1 s after the initial alert was slightly different with an updated magnitude of *M* 5.7 due to averaging of the EPIC magnitude estimates from all the ShakeAlert production servers by the SA. The final estimate of *M* 3.8 was published 4 s after the initial alert.

The location of the Truckee earthquake at the edge of the ShakeAlert seismic network made this a particularly challenging event. In addition to the lack of azimuthal coverage, which is critical for creating an accurate location estimate, this earthquake occurred in a region of low station density, which was the primary reason that FinDer did not trigger during this event.

Of the four initial stations to alert (Fig. 2), BK.WELL (38.44° N, 120.71° W; Northern California Earthquake Data Center [NCEDC], refer to Data and Resources) triggered on noise shortly before the *P* wave of the *M* 4.7 earthquake. EPIC's attempt to associate this early trigger with the rest of the good triggers caused the algorithm to push the epicentral estimate 29 km away from the true location, which in turn impacted the magnitude estimate. Furthermore, only the magnitude estimate from station CE.76140 (39.59° N, 120.37° W; Southern California Earthquake Data Center [SCEDC], refer to Data and Resources) was used in the initial magnitude estimate due to erroneous EPIC logic in place at the time. According to this logic, the code would only use the stations within 100 km if there was a station within 100 km, or, if no station was within 100 km, use only stations within 150 km if there was a station within 150 km. Stations between 150 km and the maximum distance for which station magnitude estimates are included (200 km, defined in the configuration file; maxMagKm(event) parameter) are only used if all stations are farther than 150 km. This logic was incorrect as EPIC was supposed to include triggers from any station within the distance set by the maxMagKm parameter per the

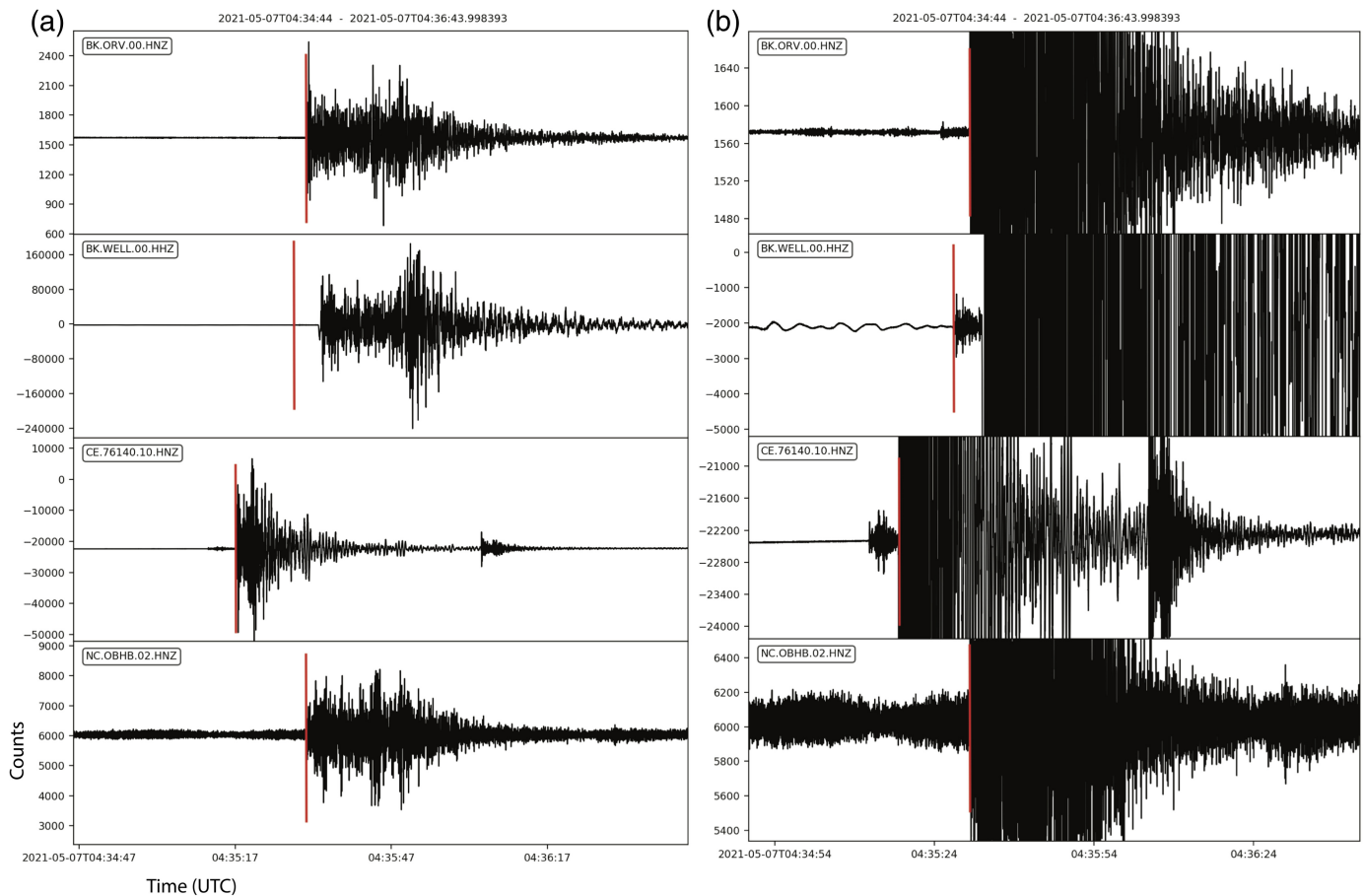


Figure 2. (a) Waveforms for the first four stations to contribute to the Earthquake Point-source Integrated Code (EPIC) solution for the 2021 **M** 4.7 Truckee earthquake (BK.ORV.HNZ, BK.WELL.HNZ, CE.76140.HNZ, and NC.OBHB.HNZ) (Northern California Earthquake Data Center [NCEDC], Southern California Earthquake Data Center [SCEDC]; refer to [Data and Resources](#)). (b) Same as left and zoomed in to EPIC triggers (red lines). The color version of this figure is available only in the electronic edition.

MaxMagDist logic. The correct logic was being used on the ShakeAlert development, test, and integration machines, and the source estimates generated by those machines were significantly more accurate than those from the production machines (Table 2). The problematic logic on the production machines was identified because of this earthquake and promptly fixed.

At the time of the Truckee earthquake, several nearby seismic stations from the Nevada seismic network (NN; refer to [Data and Resources](#)) were in the process of being added to the ShakeAlert production system. Although all ShakeAlert machines were using the same channel file (file containing all stations and channels to be used by the system), these NN stations had not yet passed the final steps of the station acceptance process, and their data were not being ingested by the production and test machines. Analysis of the log files from the development and integration machines, which were ingesting data from those stations at that time, showed that if the NN stations in the Truckee area had been used, the magnitude and location estimates of the initial alerts would have been significantly improved, with magnitude estimates ranging between **M** 4.6 and 4.8 and <1 km location error for the initial alert and all subsequent updates.

Although all of the machines with the MaxMagDist logic corrected created better magnitude estimates than the production machines for which the logic had not yet been

corrected, the development and integration machines that also used the NN stations in the first estimate and not the more distant BK.WELL station (which triggered early) created the most accurate magnitude estimates.

Shortly after this earthquake occurred, the NN stations were added to the ShakeAlert production system, which led to improvements in detection of subsequent events in that area.

2021 **M** 5.3 Calipatria earthquake

The 5 June 2021 **M** 5.3 Calipatria, California, earthquake (ComCat ID: ci39919392; [U.S. Geological Survey, Earthquake Hazards Program, 2024](#)) near the Salton Sea was a successful event for ShakeAlert as the system had both accurate magnitude and location estimates as well as a fast alert time. The initial source estimate was created by EPIC 6.7 s after the earthquake origin time with a magnitude estimate of **M** 5.2 and a location error of 1 km (Fig. 3). FinDer contributed its solution

TABLE 2

Magnitude Estimates and Location Error of EPIC Solutions for the 2021 M 4.7 Truckee Earthquake Created on the Production, Integration, Test, and Development Machines, and the Corresponding Machine Configuration Information Including Whether Stations from the Nevada Seismic Network (NN, Refer to [Data and Resources](#)) Were Used, If the Correct MaxMagDist Logic Was Being Used, Whether the New EPIC Magnitude Weighting Was Used, and If the Solution Incorporated the Early Trigger from Station BK.WELL (NCEDC, Refer to [Data and Resources](#))

Machine	Alert Time (hh:mm:ss.sss)	Magnitude	Location Error (km)	Used NN Stations?	MaxMagDist Logic Corrected?	New EPIC Magnitude Weighting?	Used Early Trigger (BK.WELL.HHZ)?
<i>bk-prod1</i>	04:35:31.959	5.99	29	No	No	No	Yes
<i>ci-prod1</i>	04:35:31.959	5.99	29	No	No	No	Yes
<i>uw-prod1</i>	04:35:31.972	5.99	29	No	No	No	Yes
bk-int1	04:35:33.060	4.66	0	Yes	Yes	No	No
ci-int1	04:35:33.126	4.66	0	Yes	Yes	No	No
uw-int1	04:35:33.115	4.66	0	Yes	Yes	No	No
<i>bk-test1</i>	04:35:32.895	4.26	29	No	Yes	No	Yes
<i>ci-test1</i>	04:35:32.033	4.17	29	No	Yes	No	Yes
<i>uw-test1</i>	04:35:31.975	4.17	29	No	Yes	No	Yes
bk-dev1	04:35:33.907	4.68	0	Yes	Yes	Yes	No
ci-dev1	04:35:33.643	4.68	0	Yes	Yes	Yes	No
uw-dev1	04:35:42.785	4.6	0	Yes	Yes	Yes	No
<i>eew2-epic1</i>	04:35:33.112	4.84	0	Yes	Yes	No	No
<i>eew2-epic2</i>	04:35:34.189	4.83	0	Yes	Yes	No	No
<i>eew2-epic6</i>	04:35:34.133	4.83	0	Yes	Yes	No	No

Italic text groups denote machines by type (prod, int, test, dev, eew2 for production, integration, test, development [Given et al., 2018](#); and EEW2 [another development machine], respectively). EEW, earthquake early warning; EPIC, Earthquake Point-source Integrated Code; NCEDC, Northern California Earthquake Data Center.

0.2 s later with a magnitude estimate of **M** 5.2 and a location error of 3 km. Magnitude estimates from both algorithms decreased slightly to **M** 5.0 1 s after the initial alert but then increased back to **M** 5.2 2.5 s later.

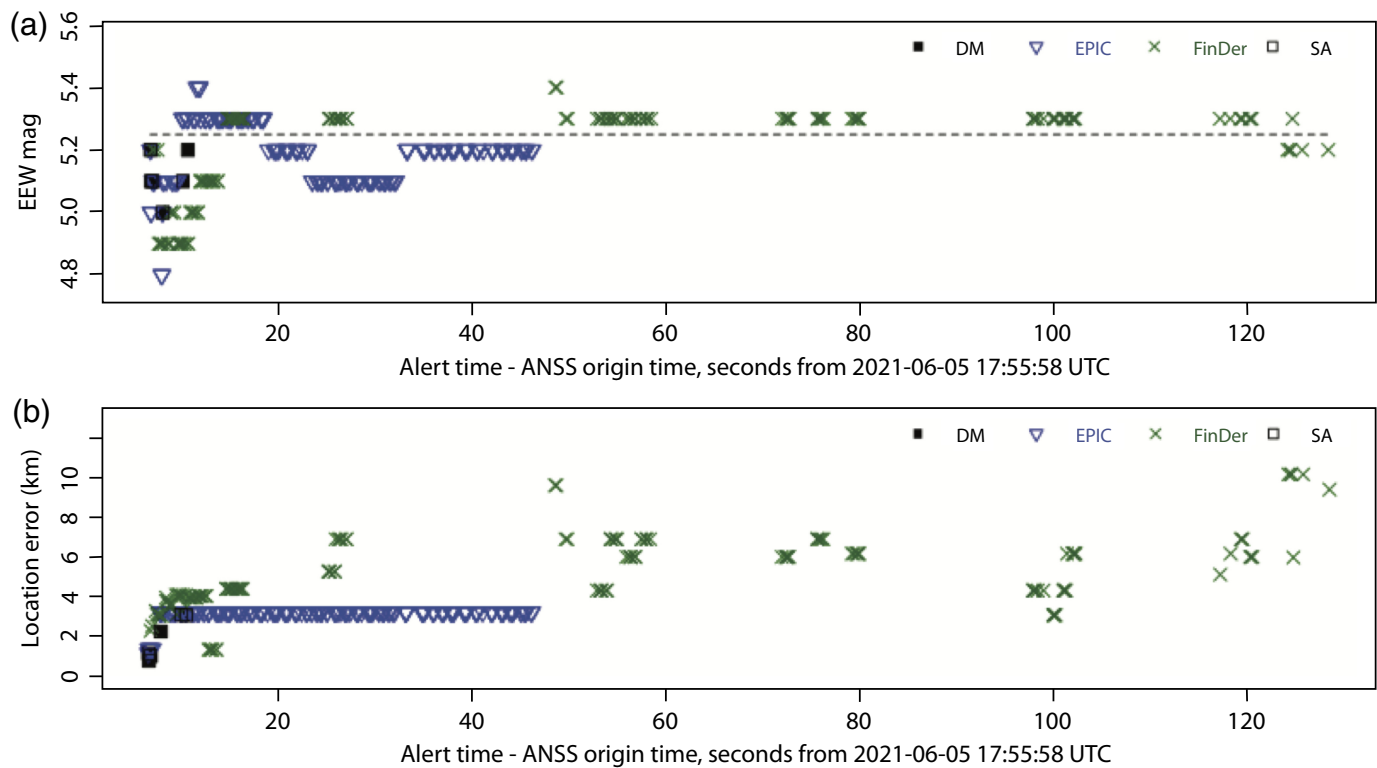
Although complex sequences of events such as foreshock and mainshock combinations or swarms of earthquakes can be challenging for ShakeAlert ([Böse, Andrews, et al., 2023](#)), the system detected most earthquakes during the swarm that occurred in the Calipatria area around the time of the **M** 5.3 earthquake. The largest earthquake that was missed during the 24 hr following the mainshock was an **M** 4.3 earthquake approximately 1.5 min after the **M** 5.3 earthquake (Table 3). ShakeAlert did not detect this earthquake because there was too much background seismic noise for EPIC to identify the *P*-wave arrival and for FinDer to create an event independent from the **M** 5.3 earthquake.

2021 M 6.0 Antelope Valley earthquake

By far the most complicated and problematic event during this reporting period was the 8 July 2021 **M** 6.0 Antelope Valley, California, earthquake (ComCat ID: 73584926; [U.S. Geological Survey, Earthquake Hazards Program, 2024](#)). The primary difficulty with this earthquake was that it occurred at the edge of the network in a region of sparse station coverage. The first stations to trigger and be associated with EPIC were a group of stations near Mammoth Lakes. Because of the density of this cluster of stations, which has been known to cause poor EPIC

location estimates, EPIC treats the group as a single station if the earthquake location is estimated to be more than 30 km from the center of the cluster (“cluster logic”), and as individual stations otherwise. However, for this event, a poor EPIC location estimate due to limited azimuthal coverage from using only stations in the Mammoth Lakes cluster located just over 100 km away brought the estimated location within the cluster, causing the stations to be treated as individual stations. As a further complication, this same process happened with a slightly different group of stations from the cluster on another ShakeAlert production machine, which caused ShakeAlert to create two different poorly located events in that area. Because this initial event location was so poor, EPIC could not associate the many other earthquake triggers that were coming into the system with this event. EPIC then associated these remaining triggers into multiple additional “split” events, one to the south of the Mammoth Lakes cluster of stations, and another 100+ km to the west. For the three split events, two had maximum magnitude estimates of **M** 4.8 and resulted in public alerts.

Although there were a few stations closer to the earthquake epicenter, EPIC did not use them in the initial solution. CI.65398 (38.77° N, 119.82° W; SCEDC, refer to [Data and Resources](#)), one of the closest stations, was not operational at the time of the earthquake. Two other nearby stations, BK.CMB (38.01° N, 120.39° W; NCEDC, refer to [Data and Resources](#)) and NN.EBPB (38.58° N, 119.81° W; NN, refer



to [Data and Resources](#)), triggered on an M 2.1 foreshock 8 s before the mainshock. Because EPIC will not allow a second trigger within 10 s of a trigger, those stations did not trigger for the mainshock.

FinDer created a single event solution 21 s after the origin time of the Antelope Valley earthquake, that is, 4.6 s faster than EPIC, with an initial magnitude estimate of M 5.3 and location error of 40 km. The magnitude estimate increased with time to a final estimate of M 5.7 7 s after the first FinDer estimate. FinDer's final line source was estimated as ~ 10 km long and striking in a north-south direction. Although the solution from FinDer could have provided an accurate public alert, it was not pushed through to the DM due to alerting rules in place at the time that prevented FinDer from creating alerts by itself. As of 23 September 2022, FinDer is now able to alert alone if its estimated magnitude is at least M 5.5.

After this earthquake, stations from the NN (Nevada) network were added to the ShakeAlert system. These stations improved the azimuthal coverage and density of the network in the region, which has led to significantly improved ShakeAlert earthquake location and magnitude estimates in the Antelope Valley area. The stations in the Mammoth Lakes area are now always treated as a cluster by EPIC.

2021 M 6.2 Petrolia earthquake

The 20 December 2021 Petrolia, California, earthquake (ComCat ID: nc73666231; [U.S. Geological Survey, Earthquake Hazards Program, 2024](#)) sequence began with an M 5.7 foreshock 24 km offshore and was followed 11 s later by an M 6.2 mainshock onshore approximately 30 km from the foreshock

Figure 3. (a) Magnitude error of alerts from EPIC, FinDer, and decision module (DM)/solution aggregator (SA) with respect to time since origin time for the 2021 M 5.3 Calipatria, California, earthquake. The horizontal dashed line represents the magnitude of ComCat (U.S. Geological Survey, Earthquake Hazards Program, 2024). (b) Location error of alerts from EPIC, FinDer, and DM/SA with respect to time since origin time for the 2021 M 5.3 Calipatria, California, earthquake. From the ShakeAlert DM review tool. The color version of this figure is available only in the electronic edition.

([Yeck et al., 2023](#)). Both ShakeAlert algorithms created alerts for this earthquake doublet, with the EPIC estimate characterizing the offshore foreshock and the FinDer solution more closely estimating the onshore mainshock.

Complex sequences with multiple earthquakes in quick succession are a known challenge for ShakeAlert ([Böse, Andrews, et al., 2023](#)). EPIC uses a short-term average/long-term average (STA/LTA) triggering algorithm to rapidly detect earthquakes ([Wurman et al., 2007](#)), which usually triggers accurately; however, it cannot trigger when there is significant noise (i.e., high LTA) at a station. When a large earthquake occurs, it is not uncommon for EPIC to not be able to detect additional earthquakes for 10 min afterward or longer. This undesirable behavior was first documented during the 2019 Ridgecrest earthquake sequence ([Chung et al., 2020](#)) when EPIC failed to detect moderate earthquakes directly following the 2019 M 6.4 and 7.1 earthquakes. After the M 7.1 Ridgecrest earthquake, for example, EPIC was not able to detect any other earthquake for 13 min, missing 13 earthquakes in the M 4.5–4.8 range during that time.

TABLE 3

ShakeAlert Performance during the Calipatria, California, Swarm (U.S. Geological Survey, Earthquake Hazards Program, 2024), Including up to 48 hr after the M 5.3 Mainshock

Origin Time (yyyy/mm/dd hh:mm:ss.sss)	ANSS Magnitude	DM Initial Magnitude	EPIC Initial Magnitude	FinDer Initial Magnitude	EPIC Initial Location Error	FinDer Initial Location Error
2021/06/07 15:58:03.420	2.4	3.6	3.6	–	15.3	
2021/06/07 14:45:22.420	3.5	–	–	–		
2021/06/07 05:44:35.620	3.6	4	4	3.3	17.1	2.4
2021/06/06 08:05:36.600	3.8	–	–	–		
2021/06/06 03:51:37.740	3.9	4	4	–	1.3	
2021/06/06 03:08:23.210	3.6	3.9	3.9	3.5	4.6	4.4
2021/06/05 19:07:07.680	2.7	3.5	3.4	–	12.7	
2021/06/05 19:05:31.380	3.3	3.7	3.7	3.4	2.6	7.4
2021/06/05 18:21:48.750	4.1	4.4	4.4	4.2	1.1	6.8
2021/06/05 18:16:14.540	2.9	3.7	3.7	3.5	13.1	5.3
2021/06/05 18:03:40.050	3.5	3.8	3.8	3.6	1.2	4.9
2021/06/05 17:57:21.900	4.3	–	–	–		
2021/06/05 17:55:58.820	5.3	5.2	5.2	5.2	1.2	2.3
2021/06/05 17:50:50.980	3.9	3.7	3.7	3.7	2	10.1
2021/06/05 17:47:53.750	3.9	–	–	–		
2021/06/05 17:46:39.500	3.8	–	–	–		
2021/06/05 17:46:26.060	3.6	–	–	–		
2021/06/05 17:45:16.380	4.1	4.5	4.5	3.7	5.9	9.5
2021/06/05 17:42:10.930	3.2	3.5	3.4	3.5	1.9	2.2
2021/06/05 17:40:51.960	3.5	–	–	–		

ANSS, Advanced National Seismic System; DM, decision module; EPIC, Earthquake Point-source Integrated Code; and FinDer, Finite-fault rupture Detector. Bold values indicate M 5.3 mainshock.

FinDer, unlike traditional methods, relies on tracking seismic-wave amplitudes instead of phase picks, making it less susceptible to background noise. This approach enabled FinDer to successfully identify four additional aftershocks ranging from M 4–5 immediately following the Ridgecrest fore- and mainshocks measuring magnitudes 6.4 and 7.1 (Chung *et al.*, 2020). However, FinDer has limitations when multiple earthquakes occur closely in time (<~120 s). For events in the same source region, such as foreshock–mainshock or mainshock–aftershock pairs, FinDer may merge them into a single detection (as in the M 6.2 Petrolia earthquake). When dealing with events in different source regions, FinDer initially processes the earlier event (if it meets the event detection criteria), but it may later switch to the event in the other source region if it generates stronger ground motions and updates its solution for the event with the new source estimate. If the updated FinDer source estimate is over 100 km away from the previous update, the new source estimate will be treated as a separate event within ShakeAlert.

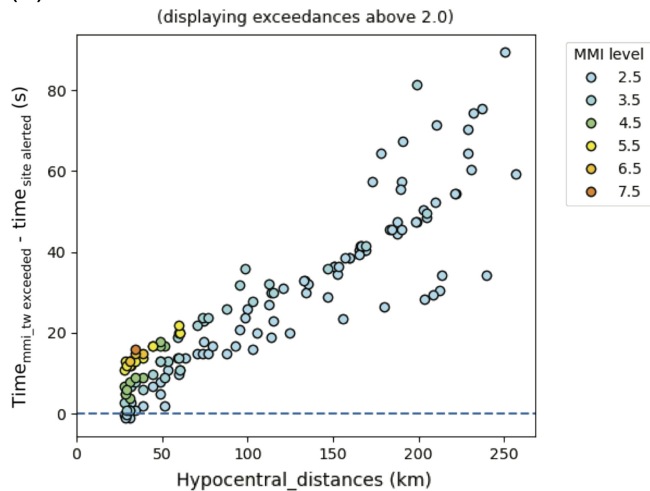
The initial ShakeAlert estimate for the 2021 M 5.7 and 6.2 Petrolia earthquake sequence came from EPIC, with an initial magnitude estimate of M 5.2 and a location error of 18 km from the M 5.7 epicenter at 8.9 s after the M 5.7 foreshock. The magnitude estimate from EPIC increased to M 5.7 4 s after the initial alert, and then decreased to M 5.4, with a final location error of less than 1 km from the foreshock’s epicenter. FinDer began contributing to alerts starting at 1 s after the first

EPIC estimate with a magnitude estimate of M 4.3 and a location error of 27 km. The FinDer magnitude estimate, which uses all waveform data available at the time of the solution in its source estimate steadily increased to a final estimate of M 6.3, very closely matching the M 6.2 Comcat mainshock magnitude and finite-source location (details on FinDer’s performance during the Petrolia earthquake are given in Böse, Andrews, Hartog, and Felizardo, 2023). These two event estimates were combined into a single event within the SA.

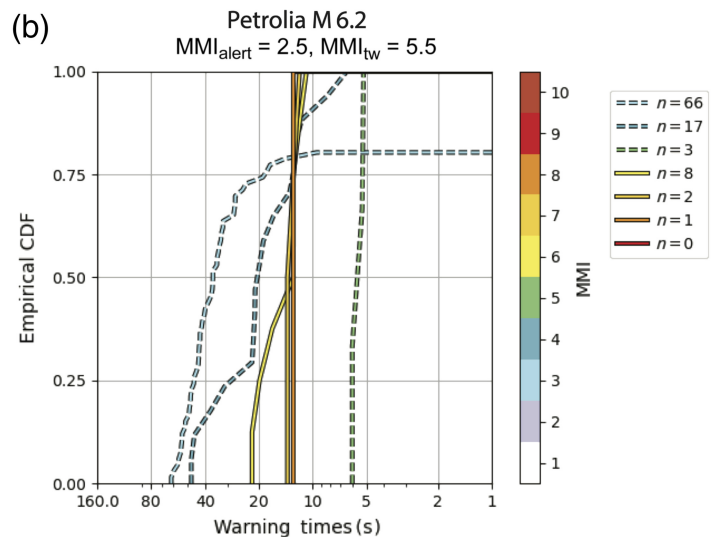
The combined SA magnitude estimate started as M 5.2 (the EPIC initial estimate), and then evolved closely following the EPIC estimate. The SA did not issue any updates associated with the M 6.2 mainshock from FinDer because of the SA combination rules at the time. This is expected behavior from the system, as the ShakeAlert logic at the time dictated that the SA more heavily weighs the EPIC location and magnitude estimates for earthquakes, with SA estimates below M 6.0. On 17 November 2022, this logic was modified such that if only the FinDer magnitude exceeds M 6 then the SA will switch to using FinDer’s magnitude. If the EPIC magnitude is above FinDer magnitude and they are both over M 6, then they will still be averaged together.

The ShakeAlert products were published 15–20 s before damaging shaking occurred at many locations. Using a low-alerting threshold of MMI 3 for cell phone apps ensures that most sites experiencing high-intensity shaking will receive

(a) Warning times for Petrolia M 6.2 at $\text{MMI}_{\text{alert}} = 2.5$



(b)



useful warnings (Minson *et al.*, 2022). Figure 4 shows warning times calculated as the time between when the ShakeAlert contour products were published and when damaging shaking (MMI 6) began as recorded at seismic stations. Although these times do not account for the delay it takes to deliver an alert, they provide maximum warning times of the system as internet-based delivery can be quite fast (median alert times <2 s in urban areas; Patel and Allen, 2022). Actual warning times for users may vary. As expected, warning times are short close to the epicenter but rapidly increase with distance. The warning time was 13 s at the only site that experienced peak shaking of MMI 8 (NP.1023: 40.58° N, 124.26° W; NP, refer to Data and Resources, MMI 7.6, warning time 12.9 s), 12–14 s for MMI 7 sites, and 11–23 s for MMI 6 sites using the MMI 3 contour alert product. Warning times for the MMI 4 contour product were slightly shorter: 13 s for the MMI 8 site, 12–14 s for MMI 7 sites, and 11–18 s for MMI 6 sites. Warning times were significantly shorter for the MMI 5 contour product for which only a few of the MMI 6 sites achieved 8 s of warning. The decrease in warning times for the MMI 5 contour product results from the time required for the magnitude estimate to increase such that MMI 5 ground motions are forecast. This was complicated by the two earthquakes that led to an absence of an onshore late alert zone for the MMI 3 and 4 contour products but poor performance for the MMI 5 contour product due to the offshore epicenter of the foreshock. The general decrease in warning times for the MMI 5 contour product due to the magnitude evolution is expected system performance based on offline simulations (McGuire *et al.*, 2021) and not due to data latency issues as experienced in the Ridgecrest sequence (Chung *et al.*, 2020).

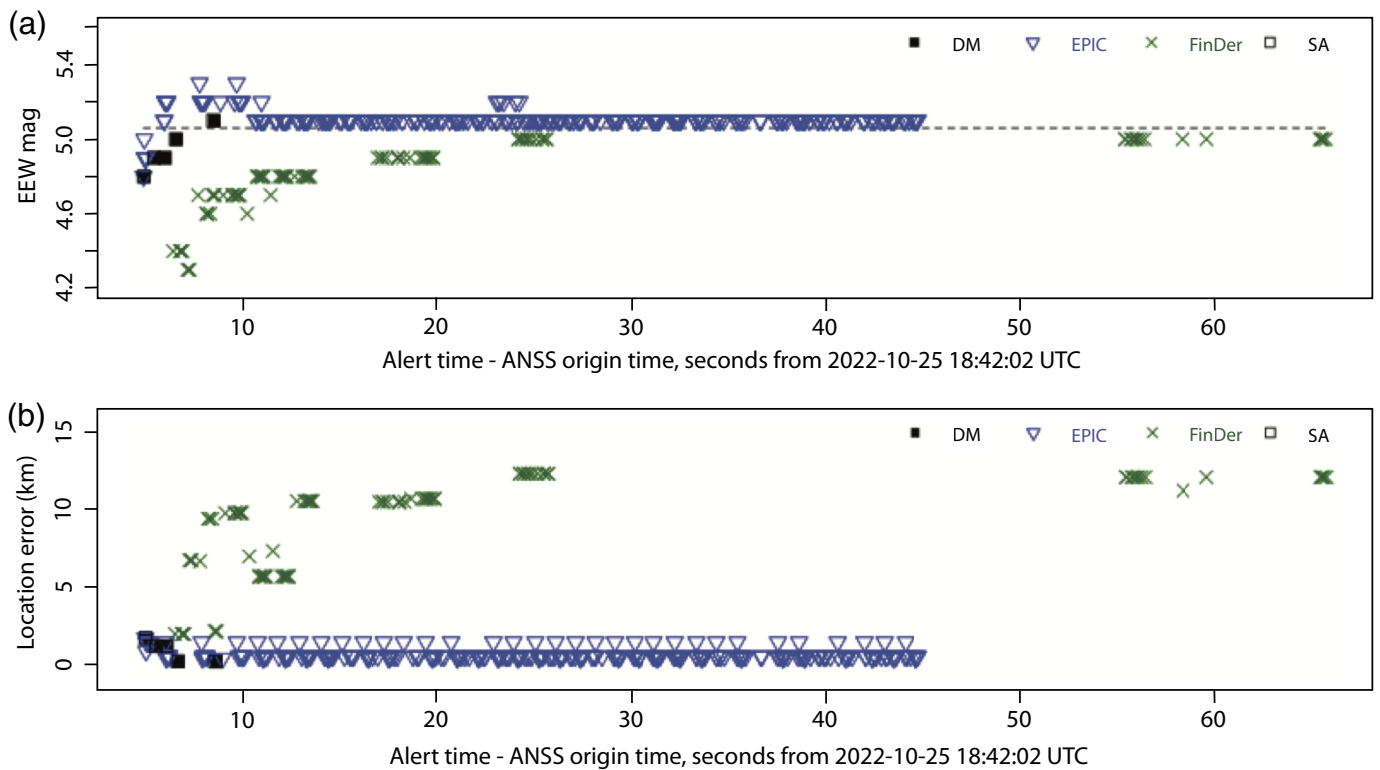
ShakeAlert created useable alerts for this very complex sequence. Because the *P* waves from the M 6.2 mainshock were embedded within the signals from the more distant M 5.7 foreshock, it was extremely unlikely that the system would be able to distinguish the two distinct earthquakes. A well-documented

Figure 4. (a) Maximum possible warning times at ShakeAlert stations as a function of hypocentral distance from the 2021 M 6.2 Petrolia earthquake, calculated using $\text{MMI}_{\text{alert}} = 2.5$ (data from networks contributing to ShakeAlert, see Data and Resources). This figure shows times at which different modified Mercalli intensity (MMI) threshold levels are exceeded by the observed ground motion at each site, relative to the earliest time when the site would hypothetically be alerted (= warning time). Each station has a symbol plotted for each MMI level that it exceeded and the highest MMI threshold for which there is a warning time measurement shows the approximate final peak ground-motion level for each site. Sites with peak observed intensities $\text{MMI}_{\text{obs}} < 2.0$ are not plotted. (b) Empirical cumulative distribution of warning times for the 2021 M 6.2 Petrolia earthquake for sites with different observed peak shaking intensities, defined using the alert time of the MMI 2.5 alert contour ($\text{MMI}_{\text{alert}} = 2.5$) and the time at which the chosen MMI warning threshold ($\text{MMI}_{\text{tw}} = 5.5$) was exceeded at a site. For sites with $\text{MMI}_{\text{alert}} \leq \text{MMI}_{\text{obs}} < \text{MMI}_{\text{tw}}$ (dashed lines), warning times are measured relative to the theoretical *S*-arrival time. Number of records per bin (*n*) are given in the figure legend. The color version of this figure is available only in the electronic edition.

limitation of EPIC's STA/LTA *P*-wave picker is that it is incapable of triggering a second earthquake if the background seismic noise is too high (e.g., immediately following a large earthquake). This earthquake highlighted the importance of utilizing estimates from two independent algorithms. Although EPIC's estimates are usually the fastest, with the more accurate location estimate, it struggles to accurately characterize multiple earthquakes in quick succession. Because of the FinDer's ability to use longer time windows of data, if a larger earthquake occurs soon after the first ShakeAlert alert, the system may still be able to create an updated solution that uses amplitude data from the second earthquake. During this event, the combined SA alert did not include updates with information about the M 6.2 earthquake from FinDer.

2022 M 5.1 Alum Rock earthquake

One of the most widespread alerts by the ShakeAlert system since the 2019 public rollout was the 25 October



2022 **M** 5.1 Alum Rock, California, earthquake (ComCat ID: nc73799091; [U.S. Geological Survey, Earthquake Hazards Program, 2024](#)). Timely alerts were widely distributed via cell phones throughout the reporting region, which included the densely populated San Francisco Bay Area. EPIC was the first algorithm to alert, producing an initial magnitude estimate of **M** 4.8 and a location error of 2 km at 5.0 s after origin time (Fig. 5). EPIC’s magnitude estimate increased slightly over the next 5 s to a final magnitude estimate of **M** 5.1, with a peak estimate of **M** 5.2. The location estimates from EPIC remained consistent with a final location error of <1 km.

FinDer contributed its first alert 2 s after the first EPIC alert with a magnitude estimate of **M** 4.4 and a location error of 2 km. The FinDer magnitude estimate increased with time, reaching a peak magnitude of **M** 5.0 at 25 s after origin time. FinDer’s first-source estimates were very close to the epicenter with later updates moving 12 km to the south, settling approximately at the center of the MMI 5 area according to the USGS ShakeMap ([Worden and Wald, 2016](#)). Because FinDer determines earthquake source parameters from the observed distribution of PGA, this migration of FinDer’s source location away from the epicenter is expected and desired behavior during earthquakes with significant rupture directivity such as the Alum Rock earthquake (e.g., [Hirakawa et al., 2023](#)).

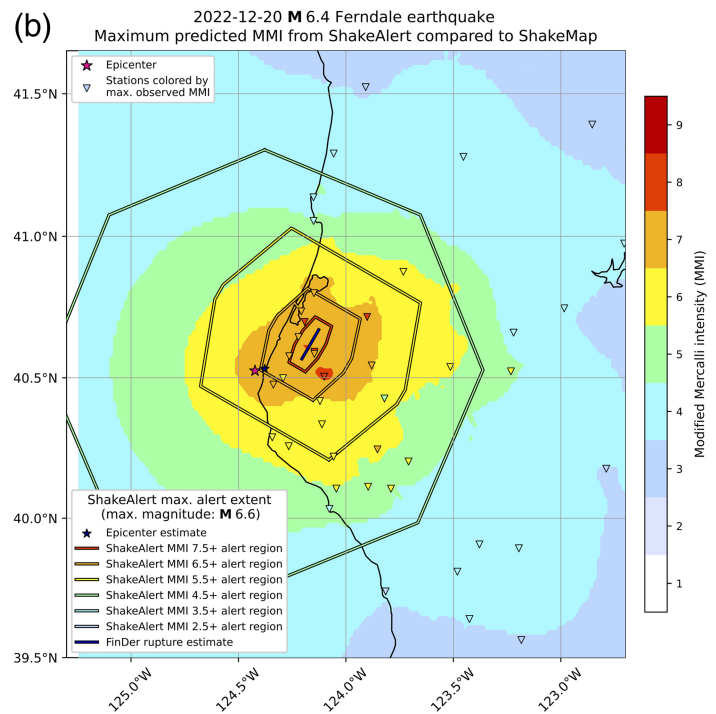
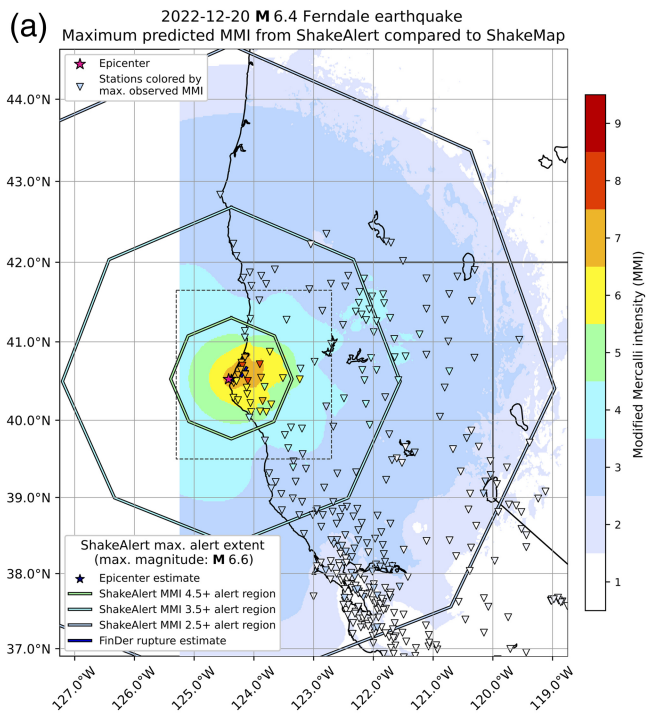
As expected for an earthquake with estimated EPIC and FinDer magnitudes both **M** <6, the SA magnitude and location estimates closely followed the EPIC estimates for the duration of this earthquake. During this event, 20% of

Figure 5. (a) Magnitude estimates of alerts from EPIC, FinDer, and DM/SA with respect to time since origin time for the 2022 **M** 5.1 Alum Rock, California, earthquake. The horizontal dashed line represents the magnitude of ComCat (U.S. Geological Survey, Earthquake Hazards Program, 2024). (b) Location error of alerts from EPIC, FinDer, and DM/SA with respect to time since origin time for the 2022 **M** 5.1 Alum Rock, California, earthquake. Figures from ShakeAlert DM review tool. The color version of this figure is available only in the electronic edition.

MyShake phones reported latencies (delay between when the alert message was received from ShakeAlert, and when the phones alerted) < 2.2 s, 50% reported latencies < 3.5 s, and 80% of phones reported latencies < 6.0 s (J. Marty, personal comm., 8 March 2024). With the rapid source estimation, fast distribution via the MyShake state-sponsored cell phone app, and the ideal location of the earthquake in the hills to the southeast of the more densely populated portions of the Bay Area, alerts were generated quickly enough for timely alerts to be distributed throughout the urbanized region.

2022 **M** 6.4 Ferndale earthquake and **M** 5.4 Rio Dell aftershock

Almost exactly 1 yr after the 2021 **M** 6.2 Petrolia earthquake, an **M** 6.4 earthquake occurred on 20 December 2022 just 18 km to the northeast of the prior earthquake near the town of Ferndale, California (ComCat ID: nc73821036; [U.S. Geological Survey, Earthquake Hazards Program, 2024](#)). ShakeAlert accurately



detected this earthquake, with both EPIC and FinDer creating accurate and timely alerts.

The first alert came into the system from EPIC 7.5 s after the earthquake origin time with an initial magnitude estimate of M 5.6 and a location error of 9.3 km. The EPIC magnitude increased to a final magnitude estimate of M 6.3 with a peak magnitude estimate of M 6.7 at 16.5 s after origin time. The EPIC location error decreased with time to a final location error of 2 km.

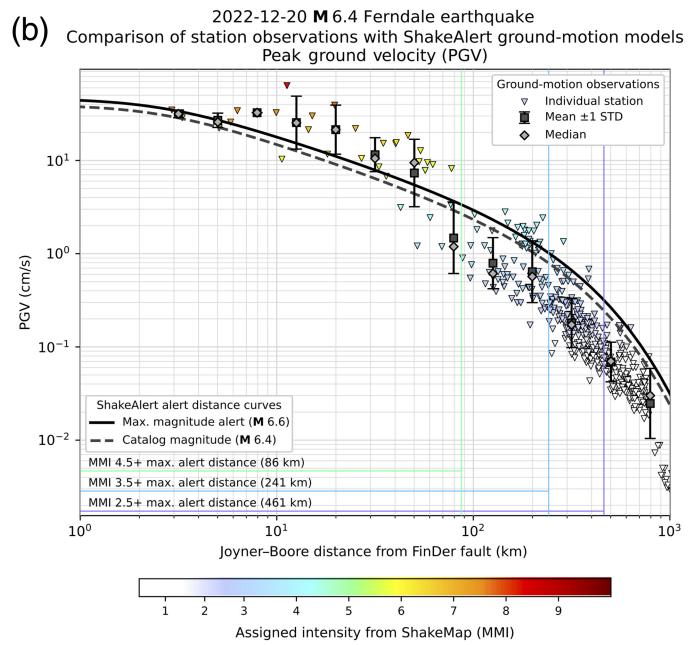
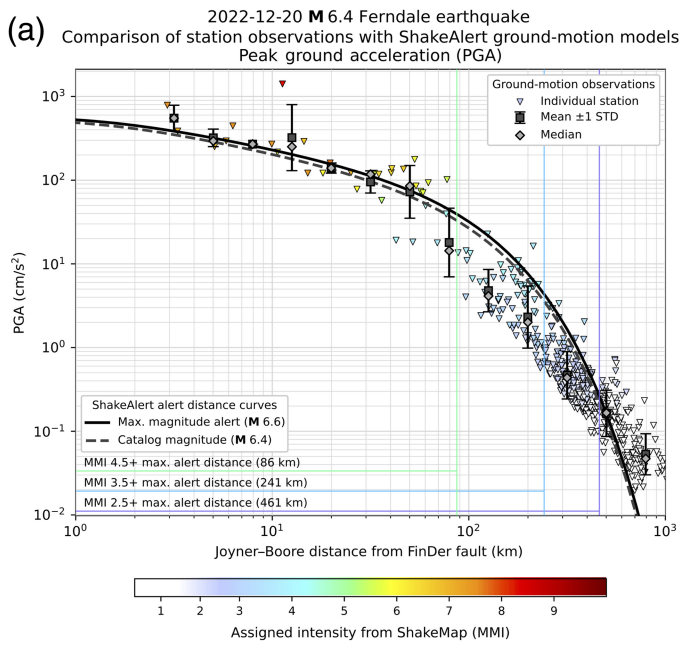
The first FinDer estimate came 0.5 s after the first EPIC estimate with an initial magnitude estimate of M 3.5, steadily increasing to a final estimate of M 6.2 at 27 s after origin time. The FinDer location error started at 11 km and increased with time to a final location error of 23 km following the pattern mentioned previously where the FinDer location estimate tracks the locations where the highest ground motions are observed. The FinDer line-source location and orientation (shown in Fig. 6) is centered on the onshore portion of $MMI \geq 7$ shaking according to the USGS ShakeMap and corresponds well with the USGS finite-source solution very well (refer to the Ferndale, California, event webpage for this event, in [Data and Resources](#)).

The SA solution closely followed the EPIC solution, with an initial magnitude estimate of M 5.6 and a location error of 9 km. The SA magnitude estimate increased to a final estimate of M 6.3 with a peak magnitude estimate of M 6.6, and the SA location error decreased with time to a final error of 2 km. Figure 6 shows the alerting polygons associated with the maximum magnitude alert. Figure 7 shows comparisons of observed PGAs and peak ground velocities with distance to the ground-motion prediction equations used by ShakeAlert

Figure 6. (a) ShakeAlert alert contours (polygons) associated with the maximum magnitude alert compared with the station MMI observations (triangles) and ShakeMap (Worden and Wald, 2016) MMI distributions (background color) for the 2022 M 6.4 Ferndale earthquake. The station observations are from the ShakeMap observation files (U.S. Geological Survey, Earthquake Hazards Program, 2024), which may be different from the stations used by ShakeAlert in real-time. (b) Same as (a) and zoomed in. The black line shows the FinDer line-source solution. Note the offset inner polygons. For $M > 6$ earthquakes, the ShakeAlert contour product will center the (shorter distance) higher MMI polygons around the FinDer line source and will center the (longer distance) lower MMI polygons around the combined SA epicenter estimate using a point-source assumption (Thakoor et al., 2019). Similar figures for other earthquakes are available in Figure S2. The color version of this figure is available only in the electronic edition.

to determine those alert regions. The ground-motion models used in ShakeAlert capture the median-observed shaking behavior well for the $MMI \geq 5$ locations for this earthquake (the ground motions of greatest interest for EEW), particularly in terms of PGV. At lower ground-motion amplitudes (distances > 100 km), there is some deviation between the ground-motion models and the station observations. This could be due to differences between the simplifying assumptions in the ShakeAlert ground-motion modeling procedure and the catalog values, for example, using an assumed 8 km source depth instead of 18 km or using an assumed stress drop rather than adjusting for an event term (e.g., Chatterjee et al., 2023).

During post-event analysis, it was discovered that the recently added “alert pause” feature had not worked properly. The alert pause is designed to prevent overalerting due to possibly erroneously high initial alerts by assigning all alerting polygons a maximum radius of 100 km for the first 5 s after



the initial alert. After the 5 s period has ended, the alert pause ends and the alert message is sent out with MMI polygons that have radii corresponding to the most recent magnitude estimate. During the 2022 Ferndale earthquake, the no alert messages with updated polygons were published after the 5 s pause ended. It was later discovered that the pause logic had been written in a way that the polygons would be updated with the first magnitude and location update after the 5 s time limit ended. However, for this event, there were no event parameter updates, and so there were also no updates to the alerting polygons. This logic has been fixed and now the updated alerting polygons are correctly published immediately after the 5 s pause as the original logic intended.

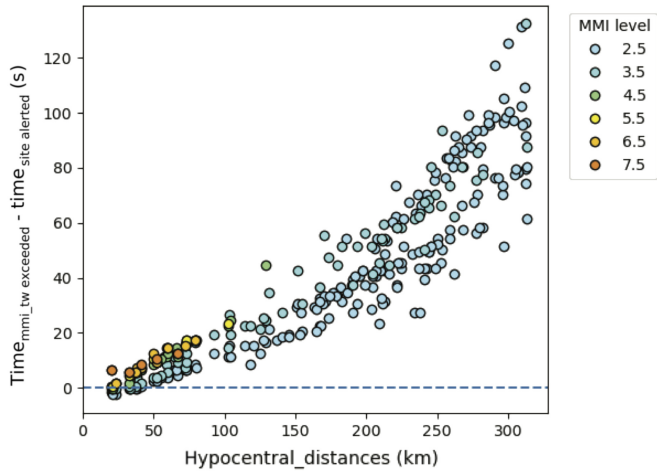
The ShakeAlert messages were published well before damaging shaking at many locations. Figure 8 shows warning times calculated between when the ShakeAlert contour products were published and when damaging shaking ($\text{MMI} \geq 6$) began as recorded at seismic stations (see also Fig. S1). Again, these do not account for the time it takes to deliver an alert but provide an upper bound on integrated system performance. As expected, warning times are small or zero seconds close to the epicenter but rapidly grow with distance. Warning times ranged from 0 to 12 s at sites that experienced peak shaking of MMI 8, 1 to 17 s for MMI 7 sites, and 0 to 23 s for MMI 6 sites using the MMI 3 contour product. Warning times for the MMI 4 contour product are identical for the $\text{MMI} \geq 6$ sites (e.g., at these distances) given the magnitude of the first alert. For the MMI 5 contour product, the warning times range from 0 to 6 s at MMI 8 sites, 0 to 10 s at MMI 7 sites, and 0 to 10 s at MMI 6 sites. Again, the decrease in warning times for the MMI 5 contour product results from the time required for the magnitude estimate to increase and is expected system performance based on offline simulations (McGuire *et al.*, 2021).

Figure 7. Comparisons of observed (a) peak ground accelerations (PGAs) and (b) peak ground velocities (PGVs) with distance to the ground-motion prediction equations used by ShakeAlert (Thakoor *et al.*, 2019) to determine alert regions for the 2022 Ferndale earthquake. The station observations are from the U.S. Geological Survey (USGS) ShakeMap observations. Station observations are colored by the MMI assigned to them by ShakeMap. These comparisons consider the ShakeAlert source estimate (magnitude, epicenter, and line source if used) associated with the peak alert from the real-time performance. The solid black line shows the ground motion with distance using the maximum magnitude estimate, and the dashed line shows the ground motion with distance using the earthquake’s catalog magnitude. The vertical-colored lines show the alert distance extents of the public alert contours (MMI V, IV, and III). Similar figures for other earthquakes are available in Figure S3. The color version of this figure is available only in the electronic edition.

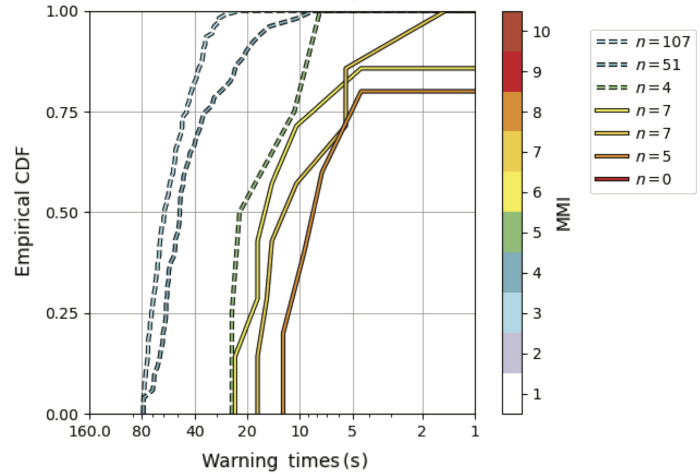
The Ferndale earthquake was followed 12 days later by an $\text{M} 5.4$ aftershock 15 km southeast of Rio Dell, California (ComCat ID: nc73827571; U.S. Geological Survey, Earthquake Hazards Program, 2024). ShakeAlert also created excellent magnitude and location estimates for this earthquake, and both EPIC and FinDer created alerts for this event. The FinDer alert came in nearly simultaneously with the EPIC first alert, though the FinDer magnitude estimates were initially underestimated. EPIC created the first alert 8.1 s after the earthquake origin time with an accurate magnitude estimate of $\text{M} 5.3$ and a location error of 2.0 km. The EPIC magnitude estimate increased slightly to a peak estimate of $\text{M} 5.6$ at 12.1 s after the origin time. The EPIC location error remained low (~ 2 km).

The first alert from FinDer came in 8.4 s after the earthquake origin time, just 0.3 s after the first alert from EPIC, with an initial magnitude estimate of $\text{M} 4.3$ and a location error of 3 km. The FinDer magnitude estimate increased to a maximum estimate of $\text{M} 5.5$ at 21.1 s after the origin time. The

(a) Warning times for Ferndale M 6.4 at $MMI_{\text{alert}} = 2.5$
(displaying exceedances above 2.0)



(b) Ferndale M 6.4
 $MMI_{\text{alert}} = 2.5, MMI_{\text{tw}} = 5.5$



location error increased quickly to 15 km at 10 s after origin time and then decreased to a final location error of 6 km. The first SA solution initially had the same magnitude and location estimates as the first EPIC alert. The addition of the lower FinDer magnitude estimate brought down the combined SA magnitude estimate slightly to M 5.0 0.6 s after the initial alert before increasing again to a peak magnitude estimate of M 5.6 at 4.7 s later. After the initial alert, the SA then settled on a final estimate of M 5.4 at 19.1 s. The SA location estimates closely followed those from EPIC.

CONCLUSIONS

Since public alerting began on 29 September 2019, there have been 53 M 4.5 and larger earthquakes that have occurred within the alerting boundary of the ShakeAlert EEW system (Fig. 1a). Of these 53 earthquakes, ShakeAlert has created matching alerts with magnitude estimates exceeding M 4.5 for 41 events (44 if the distance matching criteria are increased to 150 km instead of 100 km). Seven earthquakes that were missed by the system were all located at the edges, or outside of, the ShakeAlert seismic network. ShakeAlert detected the remaining five missed events; however, the magnitude estimates were below the alerting threshold of M 4.5. Missing 12 of the 53 earthquakes gives a missed event rate of 22.6%. Though the current missed rate of the system is higher than the performance standard that the ShakeAlert system strives for (Given *et al.*, 2018, p. 22), which states that “No more than 1 out of 10 ComCat earthquakes above the target magnitude will be missed,” a missed rate of 22.6% is ~ 2 out of 10 ComCat (U.S. Geological Survey, Earthquake Hazards Program, 2024) earthquakes that are missed, and those missed events had epicentral locations offshore, in Mexico, or at the California–Nevada border where we expect the system to struggle. The performance is better for false alerts with a false alert rate of 7.4% for the real-time system (seven false alerts out of 95 $M \geq 4.5$ alerts) compared with the 10% rate requirement

Figure 8. (a) Maximum possible warning times at ShakeAlert stations as a function of hypocentral distance from the 2022 M 6.4 Ferndale earthquake, calculated using $MMI_{\text{alert}} = 2.5$ (data from networks contributing to ShakeAlert, refer to [Data and Resources](#)). This figure shows times at which different MMI threshold levels are exceeded by the observed ground motion at each site, relative to the earliest time when the site could be alerted (= warning time). Each station has a symbol plotted for each MMI level that it exceeded and the highest MMI threshold for which there is a warning time measurement shows the approximate final peak ground-motion level for each site. Sites with peak observed intensities $MMI < 2.5$ are not plotted. (b) Empirical cumulative distribution of maximum warning times for the 2022 M 6.4 Ferndale earthquake for sites with different observed peak shaking intensities, defined using the alert time of the $MMI_{\text{alert}} = 2.5$ and the time at which $MMI_{\text{tw}} = 5.5$ was exceeded at a site. For sites with $MMI_{\text{alert}} \leq MMI_{\text{obs}} < MMI_{\text{tw}}$ (dashed lines), warning times are measured relative to the theoretical S -arrival time. Several records per bin (n) are given in the figure legend. The color version of this figure is available only in the electronic edition.

of “no more than 1 out of 10 alerts will be false” (Given *et al.*, 2018). Six of those seven events were poorly located real earthquakes. ShakeAlert created no $M \geq 5$ false alerts during this time period, and the four missed $M \geq 5$ events included the following: (1) the 2021 M 6.2 Petrolia mainshock, which occurred 11 s after an M 5.7 foreshock, for which ShakeAlert created an alert; (2) an M 5.8 offshore earthquake in 2020, also near Petrolia for which the system created an alert with an initial magnitude estimate of M 6.2 but a location estimate that was 77 km to the southwest and outside of the ShakeAlert reporting boundary and so no alert was distributed by ShakeAlert; (3) the 2021 Antelope Valley earthquake, which ShakeAlert detected but did not properly create alerts for; and (4) an M 5.1 earthquake in 2021 at the very edge of the alerting boundary in Baja, Mexico, which ShakeAlert detected with a poor location estimate.

Although the missed, false, and problematic events are not ideal, each one has provided information about how to

improve alerts. New ShakeAlert research stemming from such events includes incorporating a Bayesian approach to improve offshore and out-of-network events (Williamson *et al.*, 2023), adding a machine learning classifier to reduce false events due to spurious signals and possibly decrease alert times (Lux *et al.*, 2023), and improving FinDer ground-motion templates, including the creation of fault-specific templates that allow for modeling complex rupture geometries (Böse, Andrews, Hartog, and Felizardo, 2023, among others. Significant improvements were made following the 2019 Ridgecrest earthquakes. The EPIC magnitude underestimation during the mainshock (Chung *et al.*, 2020) led to the modification of how EPIC combines individual station magnitude estimates. Where previously magnitude estimates from all stations were averaged equally, EPIC now weights magnitude estimates from stations by the number of seconds available at each station. This improvement allows EPIC to get to higher magnitude estimates faster. Significant improvements to telemetry were also made in response to the Ridgecrest mainshock (refer to the Introduction), as well as to FinDer's handling of latent data (Böse, Andrews, Hartog, and Felizardo, 2023).

In contrast to ShakeAlert's performance during the 2019 M 7.1 and 6.4 Ridgecrest earthquakes, which produced no useable alerts for the ShakeAlertLA app (the only publicly available alert delivery cell phone app available before the public rollout in October 2019; Ruan *et al.*, 2022), the system created alerts with useful warning times for the 2022 M 6.4 Ferndale earthquake. For example, during this later earthquake, 50% of sites that recorded peak shaking of MMI 8 received alerts with warning times in excess of 10 s prior to experiencing that level of shaking (Fig. 8b). ShakeAlert has produced first alert times for all detected earthquakes in the range of 4–8 s in well-instrumented areas. These alert times continue to decrease with increasing network coverage.

Over the past 4 yr, alerting polygons corresponding to alerts published by the ShakeAlert system have covered almost all of California. Cell phone apps are the primary method of alert distribution; however, there are a variety of delivery mechanisms with different constraints. MyShake, California's official EEW cell phone app funded by the California Governor's Office of Emergency Services, has used these alerts to distribute warnings to their users in every corner of the state. Although few of the events for which alerts were created caused significant damage, the relatively low alerting threshold of the cell phone app improves the likelihood that ShakeAlert will be able to publish useful alerts during a major earthquake (Cochran *et al.*, 2019; Minson *et al.*, 2022) and also increases public awareness of the system. ShakeAlert-powered alerts have been distributed via WEA alerts for 21 earthquakes, 10 of which had ComCat (U.S. Geological Survey, Earthquake Hazards Program, 2024) magnitudes <5.0 and 11 of which had magnitudes ≥ 5.0 . These

alerts have a wide range of delivery times with many taking over 10 s (McBride *et al.*, 2023), but do not require an app download and are available to all cell phone users. The WEA delivery times can be as fast as a few seconds (McBride *et al.*, 2023) and may improve in the future.

Because it takes time to detect earthquakes and distribute the alerts, there will always be a late-alert zone near the epicenter for which no warning is possible. However, as peak ground motions for large earthquakes are often not near the epicenter due to rupture propagation and site effects, EEW can provide usable warning times to areas of potentially damaging shaking. The timeliness of warnings decreases for $\text{MMI} \geq 5$ contours, which is expected due to the time it takes for ruptures to occur and for magnitude estimates to grow such that $\text{MMI} \geq 5$ shaking is forecast. There is a trade-off between warning times and frequency of alerts, and different alert delivery mechanisms have chosen different parameter values that adjust that balance, depending on their tolerance of over- or underalerting. Overall, ShakeAlert has successfully provided warning times in excess of 10 s for larger earthquakes with the current parameter values. Warning times, as long as 10–23 s, for MMI 6–8 sites were observed in the recent M 6.4 Ferndale earthquake, and useful warning times are expected to be even more widespread in larger earthquakes.

Future ShakeAlert developments focus on improving the robustness and speed of alerts, particularly during intense earthquake sequences. Including geodetic algorithms such as G-FAST (Crowell *et al.*, 2009, 2016; Murray *et al.*, 2023) into the ShakeAlert system may lead to improved magnitude estimates (Murray *et al.*, 2023) and may provide redundancy of the system should a problem arise with the seismic networks during a large earthquake. Ground-motion-based algorithms, such as propagation of local undamped motion (Kodera *et al.*, 2018), are also being tested for possible incorporation into the ShakeAlert system. The ShakeAlert system will continue to evolve as the underlying methods are improved and rigorously tested.

ShakeAlert has created timely and accurate detections for most earthquakes that have occurred within its alerting boundary since public alerting began in 2019. Missed and poorly estimated detections have stimulated system and algorithm modifications that promise to improve detections and public alerts in the future. Because of the inherent nature of EEW, which requires fast detections and the use of very little data, there will always be a trade-off between the accuracy of ShakeAlert's source estimations and the speed of alerts. However, ShakeAlert continues to strive for detections that will meet its goal of reducing the impact of earthquakes and reducing injuries, saving lives, and property (Given *et al.*, 2018).

DECLARATION OF COMPETING INTERESTS

The authors acknowledge that there are no conflicts of interest recorded.

DATA AND RESOURCES

ShakeAlert code is governed by an intellectual property agreement among the contributing authors. ShakeAlert event summaries and parameters are available from the U.S. Geological Survey (USGS) via the network code “EW” through the National Earthquake Information Center’s (NEIC) catalog search tools, available at <https://earthquake.usgs.gov/earthquakes/search/> (last accessed September 2023). ShakeAlert website is available at <https://www.shakealert.org> (last accessed September 2023). MyShake website is available at <https://myshake.berkeley.edu> (last accessed March 2024). QuakeAlertUSA website is available at <https://earlywarninglabs.com/mobile-app/> (last accessed September 2023). Ready San Diego website is available at <https://www.readysandiego.org> (last accessed September 2023). M 6.4–15 km west-southwest of Ferndale, California, event webpage is available at <https://earthquake.usgs.gov/earthquakes/eventpage/nc73821036/executive> (last accessed December 2023). Data were obtained from the following core seismic networks: (1) the BK (Berkeley Digital Seismic Network [BDSN], 2014, operated by the UC Berkeley Seismological Laboratory, which is archived at the Northern California Earthquake Data Center [NCEDC], doi: 10.7932/NCEDC); (2) the CC (Cascade Chain Volcano Monitoring; Cascades Volcano Observatory, 2001); (3) the CE (California Strong Motion Instrumentation Program [CSMIP]; California Geological Survey, 1972); (4) the CI (Southern California Seismic Network [SCSN]; California Institute of Technology and United States Geological Survey Pasadena, 1926); (5) the CN (Canadian National Seismograph Network [CNSN]; Natural Resources Canada [NRCAN Canada], 1975); (6) the NC (Northern California Earthquake Data Center [NCEDC], UC Berkeley Seismological Laboratory, 2014, doi: 10.7932/NCEDC); (7) the IU (Global Seismographic Network [GSN]; Albuquerque Seismological Laboratory/USGS, 2014); (8) the NN (Nevada Seismic Network; University of Nevada, Reno, 1971); (9) the NP (National Strong Motion Project [NSMP]; U.S. Geological Survey, 1931); (10) the UO (PNSN-UO; University of Oregon, 1990); (11) the US (U.S. National Seismograph Network [USNSN]; Albuquerque Seismological Laboratory [ASL]/USGS, 1990); (12) the UW (PNSN; University of Washington, 1963); and (13) the WR (California Division of Water Resources). Data were also obtained from the following auxiliary seismic networks: (1) the AZ (ANZA; Vernon, 1982); (2) the BC (Red Sísmica del Noroeste de México [RESNOM]; Centro de Investigación Científica y de Educación Superior de Ensenada [CICESE], 1980); (3) the NV (North East Pacific Time-series Underwater Networked Experiments [NEPTUNE]; Ocean Networks Canada, 2009); and (4) the OO (Ocean Observatories Initiative [OOI], Rutgers University, 2013). The SCSN and the Southern California Earthquake Data Center (SCEDC) are funded through the USGS Grant G20AP00037, and the Southern California Earthquake Center, which is funded by the National Science Foundation (NSF) Cooperative Agreement EAR-0529922 and the USGS Cooperative Agreement 07HQAG0008. Waveform data, metadata, or data products for this study were accessed through the Northern California Earthquake Data Center (NCEDC), doi: 10.7932/NCEDC. ABC7 News. City of Los Angeles phasing out ShakeAlertLA in favor of new app, MyShake, available at <https://abc7.com/usgs-earthquakes-california-shakealert/9043185/> (last accessed March 2024). The Comprehensive Catalog (ComCat) earthquake source information, ShakeMaps, and ShakeMap station observations were obtained from

the USGS (USGS, 2017, last accessed January 2024). The supplemental material contains seismograms for the 2022 M 6.4 Ferndale earthquake depicting warning time until strong shaking occurs and additional performance figures for each earthquake described in the [System Performance](#) section. The supplemental material also contains a csv file containing ComCat (U.S. Geological Survey, Earthquake Hazards Program, 2024) and ShakeAlert decision module (DM; Given *et al.*, 2018) data used in this study.

ACKNOWLEDGMENTS

This material is based upon work supported by the U.S. Geological Survey (USGS) under Grant/Cooperative Agreement Number G21AC10525 to UC Berkeley, Number G21AC10532 to the Eidgenössische Technische Hochschule (ETH) Zürich, Number G21AC10561 to the California Institute of Technology (Caltech), Number G21AC10526 to University of Oregon, and Number G21AC10529 to University of Washington. The authors would like to thank the associate editor, two anonymous reviewers, and Jessica Murray, Grace Parker, and Valerie Thomas for their constructive comments that helped improve this article. ShakeAlert is a registered trademark of the USGS-managed ShakeAlert Earthquake Early Warning System operating in the United States of America and is used with permission.

Any use of trade, firm, or product names is for descriptive purposes only and does not imply endorsement by the U.S. Government.

REFERENCES

- Adams, R. M., J. Tobin, L. Peek, J. Breeden, S. McBride, and R. de Groot (2022). The generational gap: Children, adults, and protective actions in response to earthquakes, *Australas. J. Disaster Trauma Stud.* **26**, no. 2, 67–82.
- Albuquerque Seismological Laboratory/USGS (2014). Global Seismograph Network (GSN - IRIS/USGS) (Dataset), *International Federation of Digital Seismograph Networks*, doi: 10.7914/SN/IU.
- Albuquerque Seismological Laboratory (ASL)/USGS (1990). United States National Seismic Network (Dataset), *International Federation of Digital Seismograph Networks*, doi: 10.7914/SN/US.
- Allen, R. M. (2007). The ElarmS earthquake early warning methodology and application across California, *Earthq. Early Warn. Syst.* **2003**, 21–43, doi: 10.1007/978-3-540-72241-0_3.
- Allen, R. M., and H. Kanamori (2003). The potential for earthquake early warning in southern California, *Science* **300**, no. 5620, 786–789, doi: 10.1126/science.1080912.
- Allen, R. M., and M. Stogaitis (2022). Global growth of earthquake early warning, *Science* **375**, no. 6582, 717–718.
- Allen, R. M., P. Gasparini, O. Kamigaichi, and M. Böse (2009). The status of earthquake early warning around the world: An introductory overview, *Seismol. Res. Lett.* **80**, no. 5, 682–693, doi: 10.1785/gssrl.80.5.682.
- Allen, R. M., Q. Kong, and R. Martin-Short (2019). The MyShake platform: A global vision for earthquake early warning, *Pure Appl. Geophys.* **117**, 1699–1712.
- Antoniades, D., M. Athanatos, A. Papadogiannakis, E. P. Markatos, and C. Dovrolis (2006). Available bandwidth measurement as simple as running wget, *Proc. of the Passive and Active Measurements*, March 2006.

- Atkinson, G. M., and D. M. Boore (2011). Modifications to existing ground-motion prediction equations in light of new data, *Bull. Seismol. Soc. Am.* **101**, no. 3, 1121–1135.
- Berkeley Digital Seismic Network (BDSN) (2014). Berkeley digital seismic network, *UC Berkeley Seismological Laboratory*, Dataset, doi: [10.7932/BDSN](https://doi.org/10.7932/BDSN).
- Boore, D. M., and G. M. Atkinson (2008). Ground-motion prediction equations for the average horizontal component of PGA, PGV, and 5%-Damped PSA at spectral periods between 0.01 s and 10.0 s, *Earthq. Spectra* **24**, no. 1, 99–138, doi: [10.1193/1.2830434](https://doi.org/10.1193/1.2830434).
- Böse, M., R. Allen, H. Brown, G. Gua, M. Fischer, E. Hauksson, T. Heaton, M. Hellweg, M. Liukis, D. Neuhauser, *et al.* (2014). CISM ShakeAlert: An earthquake early warning demonstration system for California, in *Early Warning for Geological Disasters*, F. Wenzel and J. Zschau (Editors), Scientific Methods and Current Practice, Springer, Berlin, Heidelberg, 49–69.
- Böse, M., J. Andrews, R. Hartog, and C. Felizardo (2023). Performance and next generation development of the finite-fault rupture detector (FinDer) within the United States West Coast ShakeAlert warning system, *Bull. Seismol. Soc. Am.* **113**, no. 2, 648–663, doi: [10.1785/0120220183](https://doi.org/10.1785/0120220183).
- Böse, M., J. Andrews, C. O'Rourke, D. Kilb, A. Lux, J. Bunn, and J. McGuire (2023). Testing the ShakeAlert earthquake early warning system using synthesized earthquake sequences, *Seismol. Res. Lett.* **94**, no. 1, 243–259, doi: [10.1785/0220220088](https://doi.org/10.1785/0220220088).
- Böse, M., C. Felizardo, and T. H. Heaton (2015). Finite-fault rupture detector (FinDer): Going real-time in California ShakeAlert warning system, *Seismol. Res. Lett.* **86**, 1692–1704, doi: [10.1785/0220150154](https://doi.org/10.1785/0220150154).
- Böse, M., E. Hauksson, K. Solanki, H. Kanamori, and T. H. Heaton (2009). Real-time testing of the on-site warning algorithm in southern California and its performance during the July 29 2008 Mw 5.4 Chino Hills earthquake, *Geophys. Res. Lett.* **36**, L00B03, doi: [10.1029/2008GL036366](https://doi.org/10.1029/2008GL036366).
- Böse, M., E. Hauksson, K. Solanki, H. Kanamori, Y. M. Wu, and T. H. Heaton (2009). A new trigger criterion for improved real-time performance of onsite earthquake early warning in southern California, *Bull. Seismol. Soc. Am.* **99**, no. 2A, 897–905, doi: [10.1785/0120080034](https://doi.org/10.1785/0120080034).
- Böse, M., T. H. Heaton, and E. Hauksson (2012). Real-time finite fault rupture detector (FinDer) for large earthquakes, *Geophys. J. Int.* **191**, no. 2, 803–812, doi: [10.1111/j.1365-246X.2012.05657.x](https://doi.org/10.1111/j.1365-246X.2012.05657.x).
- Böse, M., D. Smith, C. Felizardo, M.-A. Meier, T. H. Heaton, and J. Clinton (2018). FinDer v. 2: Improved real-time ground-motion predictions for M2–M9 with seismic finite-source characterization, *Geophys. J. Int.* **212**, no. 1, 725–742.
- Bostrom, A., S. K. McBride, J. S. Becker, J. D. Goltz, R. M. de Groot, L. Peek, B. Terbush, and M. Dixon (2022). Great expectations for earthquake early warnings on the United States West Coast, *Int. J. Disaster Risk Reduct.* **82**, 103,296.
- Brown, H. M., R. M. Allen, M. Hellweg, O. Khainovski, D. Neuhauser, and A. Souf (2011). Development of the ElarmS methodology for earthquake early warning: Realtime application in California and offline testing in Japan, *Soil Dynam. Earthq. Eng.* **31**, 188–200.
- California Geological Survey (1972). California strong motion instrumentation program (Dataset), *International Federation of Digital Seismograph Networks*, doi: [10.7914/b34q-bb70](https://doi.org/10.7914/b34q-bb70).
- California Institute of Technology and United States Geological Survey Pasadena (1926). Southern California Seismic Network (Dataset), *International Federation of Digital Seismograph Networks*, doi: [10.7914/SN/CI](https://doi.org/10.7914/SN/CI).
- Cascades Volcano Observatory/USGS (2001). Cascade Chain volcano monitoring (Dataset), *International Federation of Digital Seismograph Networks*, doi: [10.7914/SN/CC](https://doi.org/10.7914/SN/CC).
- Centro de Investigación Científica y de Educación Superior de Ensenada (CICESE), Ensenada (1980). Red Sísmica del Noroeste de México (Dataset), *International Federation of Digital Seismograph Networks*, doi: [10.7914/SN/BC](https://doi.org/10.7914/SN/BC) (in Spanish).
- Chatterjee, A., N. Igonin, and D. T. Trugman (2023). A real-time and data-driven ground-motion prediction framework for earthquake early warning, *Bull. Seismol. Soc. Am.* **113**, no. 2, 676–689.
- Chiou, B.-J., and R. R. Youngs (2008). An NGA Model for the average horizontal component of peak ground motion and response spectra, *Earthq. Spectra* **24**, no. 1, 173–215, doi: [10.1193/1.2894832](https://doi.org/10.1193/1.2894832).
- Chung, A. I., I. Henson, and R. M. Allen (2019). Optimizing earthquake early warning performance: ElarmS-3, *Seismol. Res. Lett.* **90**, no. 2A, doi: [10.1785/0220180192](https://doi.org/10.1785/0220180192).
- Chung, A. I., M.-A. Meier, J. Andrews, M. Böse, B. W. Crowell, J. J. McGuire, and D. E. Smith (2020). ShakeAlert earthquake early warning system performance during the 2019 Ridgecrest earthquake sequence, *Bull. Seismol. Soc. Am.* **110**, no. 4, 1904–1923.
- Cochran, E. S., J. Bunn, S. E. Minson, A. S. Baltay, D. L. Kilb, Y. Kodera, and M. Hoshiba (2019). Event detection performance of the PLUM earthquake early warning algorithm in Southern California, *Bull. Seismol. Soc. Am.* **109**, no. 4, 1524–1541, doi: [10.1785/0120180326](https://doi.org/10.1785/0120180326).
- Cochran, E. S., M. D. Kohler, D. D. Given, S. Guiwits, J. Andrews, M.-A. Meier, M. Ahmad, I. Henson, R. Hartog, and D. Smith (2018). Earthquake early warning ShakeAlert system: Testing and certification platform, *Seismol. Res. Lett.* **89**, no. 1, 108–117, doi: [10.1785/0220170138](https://doi.org/10.1785/0220170138).
- Crane, S. J., H. Seywerd, J. Adams, A. Bird, M. Kolaj, and H. K. C. Perry (2023). National earthquake early warning for Canada, *Canadian Conference – Pacific Conference on Earthquake Engineering 2023*, Vancouver, British Columbia, Paper ID 126–1.
- Crayne, J., C. Herrán, D. F. Sumy, M. Benne, T. Shagott, and L. Peek (2023). Public education about ShakeAlert® earthquake early warning: evaluation of an animated video in English and Spanish, *Int. J. Sci. Edu. Part B* **14**, 232–256.
- Crowell, B. W., Y. Bock, and M. B. Squibb (2009). Demonstration of earthquake early warning using total displacement waveforms from real-time GPS networks, *Seismol. Res. Lett.* **80**, no. 5, 772–782, doi: [10.1785/gssrl.80.5.772](https://doi.org/10.1785/gssrl.80.5.772).
- Crowell, B. W., D. A. Schmidt, P. Bodin, J. E. Vidale, J. Gomberg, J. R. Hartog, V. C. Kress, T. I. Melbourne, M. Santillan, S. E. Minson, *et al.* (2016). Demonstration of the Cascadia G-FAST geodetic earthquake early warning system for the Nisqually, Washington, earthquake, *Seismol. Res. Lett.* **87**, no. 4, 930–943, doi: [10.1785/0220150255](https://doi.org/10.1785/0220150255).
- Cua, G. B., and T. Heaton (2007). The virtual seismologist (VS) method: A Bayesian approach to earthquake early warning, in *Earthquake Early Warning Systems*, P. Gasparini, G. Manfredi, and J. Zschau (Editors), Springer, Berlin, Heidelberg, 97–132.
- Cua, G. B., M. Fischer, T. Heaton, and S. Wiemer (2009). Real-time performance of the virtual seismologist earthquake early warning

- algorithm in Southern California, *Seismol. Res. Lett.* **80**, no. 5, 740–747, doi: [10.1785/gssrl.80.5.740](https://doi.org/10.1785/gssrl.80.5.740).
- de Groot, R. M., D. F. Sumy, S. K. McBride, M. R. Jenkins, G. Lotto, M. Vinci, and S. Olds (2022). ShakeAlert: A people-focused earthquake early warning system, *Proc. of the 12th National Conf. on Earthquake Engineering*, Vol. 27.
- 2** FEMA (2024, August 2). *Wireless Emergency Alerts*. Available at <https://www.fema.gov/emergency-managers/practitioners/integrated-public-alert-warning-system/public/wireless-emergency-alerts>.
- Given, D. D., R. M. Allen, A. S. Baltay, P. Bodin, E. S. Cochran, K. Creager, R. M. de Groot, L. S. Gee, E. Hauksson, T. H. Heaton, *et al.* (2018). Revised technical implementation plan for the ShakeAlert system—An earthquake early warning system for the West Coast of the United States, *U.S. Geol. Surv. Open-File Rept. No. 2018-1155*.
- Goltz, J. D. (2023). Social science contributions to earthquake warnings: Commemorating the work of Dennis S. Mileti, *Nat. Hazards Rev.* **24**, no. 2, 03123003, doi: [10.1061/NHREFO.NHENG-1697](https://doi.org/10.1061/NHREFO.NHENG-1697).
- Guy, M., J. Patton, J. M. Fee, M. Hearne, E. M. Martinez, D. Ketchum, C. B. Worden, V. Quitoriano, E. J. Hunter, G. M. Smoczyk, *et al.* (2015). National Earthquake Information Center systems overview and integration, *U.S. Geol. Surv. Open-File Rept. 2015-1120*, 25 pp., doi: [10.3133/ofr20151120](https://doi.org/10.3133/ofr20151120).
- Hirakawa, E., G. A. Parker, A. Baltay, and T. Hanks (2023). Rupture directivity of the 25 October 2022 5.1 Alum Rock earthquake, *Seism. Record*, **3**, no. 2, 144–155. doi: [10.1785/0320230013](https://doi.org/10.1785/0320230013).
- Jain, M., and C. Dovrolis (2003). End-to-end available bandwidth: Measurement methodology, dynamics, and relation with TCP throughput, *IEEE/ACM Trans. Netw.* **11**, no. 4, 537–549.
- Jenkins, M. R., S. K. McBride, M. Morgoch, and H. Smith (2022). Considerations for creating equitable and inclusive communication campaigns associated with ShakeAlert, the earthquake early warning system for the West Coast of the USA, *Disaster Prev. Manag.* **31**, no. 1, 79–91.
- Kanamori, H. (2005). Real-time seismology and earthquake damage mitigation, *Annu. Rev. Earth Planet. Sci.* **33**, no. 1, 195–214, doi: [10.1146/annurev.earth.33.092203.122626](https://doi.org/10.1146/annurev.earth.33.092203.122626).
- Kodera, Y., Y. Yamada, K. Hirano, K. Tamaribuchi, S. Adachi, N. Hayashimoto, M. Morimoto, M. Nakamura, and M. Hoshiba (2018). The propagation of local undamped motion (PLUM) method: A simple and robust seismic wavefield estimation approach for earthquake early warning, *Bull. Seismol. Soc. Am.* **108**, no. 2, 983–1003, doi: [10.1785/0120170085](https://doi.org/10.1785/0120170085).
- Kohler, M. D., D. E. Smith, J. Andrews, A. I. Chung, R. Hartog, I. Henson, D. D. Given, R. de Groot, and S. Guiwits (2020). Earthquake early warning ShakeAlert 2.0: Public Rollout, *Seismol. Res. Lett.* **91**, 1763–1775, doi: [10.1785/0220190245](https://doi.org/10.1785/0220190245).
- Kohler, M. D., E. S. Cochran, D. Given, S. Guiwits, D. Neuhauser, I. Henson, R. Hartog, P. Bodin, V. Kress, S. Thompson, *et al.* (2018). Earthquake early warning ShakeAlert System: West Coast wide production prototype, *Seismol. Res. Lett.* **89**, 99–107, doi: [10.1785/0220170140](https://doi.org/10.1785/0220170140).
- Kuyuk, H. S., R. M. Allen, H. Brown, M. Hellweg, I. Henson, and D. Neuhauser (2014). Designing a network-based earthquake early warning algorithm for California: ElarmS-2, *Bull. Seismol. Soc. Am.* **104**, no. 1, 162–173.
- Lin, R.-G. (2019). New earthquake early warning app for California is unveiled, *Los Angeles Times*, available at <https://www.latimes.com/local/lanow/la-me-ln-earthquake-early-warning-app-20190102-story.html> (last accessed August 2024).
- Lux, A. I., I. Henson, A. Williamson, M.-A. Meier, and R. M. Meier (2023). EPIC earthquake early warning algorithm: Recent performance and improvements, *Poster Presentation at 2023 AGU Annual Meeting*.
- McBride, S. K., and R. M. DeGroot (2023). Social Science and ShakeAlert, the earthquake early warning system for the West Coast of the United States, *Proc. of the Paper presented at the Basin and Range Conference in Salt Lake City*, Utah, October 2022.
- McBride, S. K., A. Bostrom, J. Sutton, R. M. de Groot, A. S. Baltay, B. Terbush, P. Bodin, M. Dixon, E. Holland, R. Arba, *et al.* (2020). Developing post-alert messaging for ShakeAlert, the earthquake early warning system for the West Coast of the United States of America, *Int. J. Disaster Risk Reduct.* **50**, 101,713.
- McBride, S. K., H. Smith, M. Morgoch, D. Sumy, M. Jenkins, L. Peek, A. Bostrom, D. Baldwin, E. Reddy, R. de Groot, *et al.* (2022). Evidence-based guidelines for protective actions and earthquake early warning systems, *Geophysics* **87**, no. 1, WA77–WA102.
- McBride, S. K., D. F. Sumy, A. L. Llenos, G. A. Parker, J. McGuire, J. K. Saunders, M.-A. Meier, P. Schuback, D. Given, and R. de Groot (2023). Latency and geofence testing of wireless emergency alerts intended for the ShakeAlert® earthquake early warning system for the West Coast of the United States of America, *Safety Sci.* **157**, 105,898.
- McGuire, J. J., D. E. Smith, A. D. Frankel, E. A. Wirth, S. K. McBride, and R. M. de Groot (2021). Expected warning times from the ShakeAlert earthquake early warning system for earthquakes in the Pacific Northwest (ver. 1.1, March 24, 2021), *U.S. Geol. Surv. Open-File Rept. 2021-1026*, 37 pp., doi: [10.3133/ofr20211026](https://doi.org/10.3133/ofr20211026).
- Minson, S. E., E. S. Cochran, J. K. Saunders, S. K. McBride, S. Wu, A. S. Baltay, and K. R. Milner (2022). What to expect when you are expecting earthquake early warning, *Geophys. J. Int.* **231**, 1386–1403, doi: [10.1093/gji/ggac246](https://doi.org/10.1093/gji/ggac246).
- Murray, J. R., B. W. Crowell, M. H. Murray, C. W. Ulberg, J. J. McGuire, M. A. Aranha, and M. T. Hagerty (2023). Incorporation of real-time earthquake magnitudes estimated via peak ground displacement scaling in the ShakeAlert earthquake early warning system, *Bull. Seismol. Soc. Am.* **113**, no. 3, 1286–1310.
- Natural Resources Canada (NRCAN Canada) (1975). Canadian National Seismograph Network (Dataset), *International Federation of Digital Seismograph Networks*, doi: [10.7914/SN/CN](https://doi.org/10.7914/SN/CN).
- Northern California Earthquake Data Center (NCEDC) (2014a). Northern California earthquake data center, *UC Berkeley Seismological Laboratory*, Dataset, doi: [10.7932/NCEDC](https://doi.org/10.7932/NCEDC).
- NCEDC (2014b). Berkeley Digital Seismic Network (BDSN) (Dataset), *Northern California Earthquake Data Center*, doi: [10.7932/BDSN](https://doi.org/10.7932/BDSN).
- Ocean Networks Canada (2009). NEPTUNE seismic stations (Dataset), *International Federation of Digital Seismograph Networks*, doi: [10.7914/SN/NV](https://doi.org/10.7914/SN/NV).
- Patel, S. C., and R. M. Allen (2022). The MyShake App: User experience of early warning delivery and earthquake shaking, *Seismol. Res. Lett.* **93**, no. 6, 3324–3336, doi: [10.1785/0220220062](https://doi.org/10.1785/0220220062).
- Ruan, T., Q. Kong, S. K. McBride, A. Sethjiwala, and Q. Lv (2022). Cross-platform analysis of public responses to the 2019 Ridgecrest earthquake sequence on Twitter and Reddit, *Sci. Rep.* **12**, no. 1, 1634.

- Rutgers University (2013). Ocean observatories initiative (Dataset), *International Federation of Digital Seismograph Networks*, doi: [10.7914/SN/OO](https://doi.org/10.7914/SN/OO).
- Steim, J. M., and E. N. Spassov, (2017). On data latency and compression, available at <https://www.kinematics.com/wp-content/uploads/2017/05/on-data-latency-and-compression.pdf> (last accessed August 2024).
- Stubailo, I., M. Alvarez, G. Biasi, R. Bhadha, and E. Hauksson (2020). Latency of waveform data delivery from the southern California seismic network during the 2019 Ridgecrest earthquake sequence and its effect on ShakeAlert, *Seismol. Res. Lett.* **92**, 170–186, doi: [10.1785/0220200211](https://doi.org/10.1785/0220200211).
- Stubailo, I., R. Bhadha, M. Watkins, M. Alvarez, G. Biasi, and A. Husker (2023). Redundant telemetry, system monitoring, and planning tools for a highly resilient and secure regional seismic network (RSN), *Poster Presentation at 2023 SSA Annual Meeting*.
- Sumy, D. F., O. O. Drakes, S. K. McBride, and M. R. Jenkins (2023). Social vulnerability and geographic access barriers to earthquake early warning education in museums and other free choice learning environments, *Int. J. Disaster Risk Reduct.* **97**, 104,011.
- Sumy, D. F., M. R. Jenkins, J. Crayne, S. E. Olds, M. L. Anderson, J. Johnson, B. Magura, C. L. Pridmore, and R. M. de Groot (2022). Education initiatives to support earthquake early warning: A retrospective and a roadmap, *Seismol. Res. Lett.* **93**, no. 6, 3498–3513.
- Sumy, D. F., M. R. Jenkins, S. K. McBride, and R. M. de Groot (2022). Typology development of earthquake displays in free-choice learning environments, to inform earthquake early warning education in the United States, *Int. J. Disaster Risk Reduct.* **73**, 102,802.
- Sutton, J., M. M. Wood, S. Crouch, and N. Waugh (2023). Public perceptions of US earthquake early warning post-alert messages: Findings from focus groups and interviews, *Int. J. Disaster Risk Reduct.* **84**, 103,488.
- Thakoor, K., J. Andrews, E. Hauksson, and T. Heaton (2019). From earthquake source parameters to ground-motion warnings near you: The ShakeAlert earthquake information to ground-motion (eqInfo2GM) method, *Seismol. Res. Lett.* **90**, no. 3, 1243–1257.
- University of Nevada, Reno (1971). Nevada Seismic Network (Dataset), *International Federation of Digital Seismograph Networks*, doi: [10.7914/SN/NN](https://doi.org/10.7914/SN/NN).
- University of Oregon (1990). Pacific Northwest Seismic Network - University of Oregon (Dataset), *International Federation of Digital Seismograph Networks*, doi: [10.7914/SN/UO](https://doi.org/10.7914/SN/UO).
- University of Washington (1963). Pacific Northwest Seismic Network - University of Washington (Dataset), *International Federation of Digital Seismograph Networks*, doi: [10.7914/SN/UW](https://doi.org/10.7914/SN/UW).
- U.S. Geological Survey (1931). United States National Strong-Motion Network (Dataset), *International Federation of Digital Seismograph Networks*, doi: [10.7914/SN/NP](https://doi.org/10.7914/SN/NP).
- U.S. Geological Survey (2024). Entire U.S. West coast now has access to ShakeAlert®, available at <https://www.usgs.gov/news/entire-us-west-coast-now-has-access-shakealert-earthquake-early-warning> (last accessed March 2024).
- U.S. Geological Survey, Earthquake Hazards Program (2024). Advanced National Seismic System (ANSS) comprehensive catalog of earthquake events and products: Various, doi: [10.5066/F7MS3QZH](https://doi.org/10.5066/F7MS3QZH).
- Vernon, F. (1982). ANZA Regional Network [Data set], *International Federation of Digital Seismograph Networks*, doi: [10.7914/SN/AZ](https://doi.org/10.7914/SN/AZ).
- Wald, D. J., V. Quintoriano, T. H. Heaton, and H. Kanamori (1999). Relationships between peak ground acceleration, peak ground velocity, and modified Mercalli intensity in California, *Earthq. Spectra* **15**, no. 3, 557–564.
- Williamson, A., A. Lux, and R. Allen (2023). Improving out of network earthquake locations using prior seismicity for use in earthquake early warning, *Bull. Seismol. Soc. Am.* **113**, 664–675, doi: [10.1785/0120220159](https://doi.org/10.1785/0120220159).
- Woolfolk, J. (2023). This early-warning earthquake app has been retired, but here are others that Californians can still rely on, *The Mercury News*, available at <https://www.mercurynews.com/2023/11/07/this-early-warning-earthquake-app-has-been-retired-but-here-are-others-that-californians-can-still-rely-on/> (last accessed March 2024).
- Worden, C., M. Gerstenberger, D. Rhoades, and D. Wald (2012). Probabilistic relationships between ground-motion parameters and modified Mercalli intensity in California, *Bull. Seismol. Soc. Am.* **102**, 204–221, doi: [10.1785/0120110156](https://doi.org/10.1785/0120110156).
- Worden, C. B., and D. J. Wald (2016). ShakeMap manual online: Technical manual, user’s guide, and software guide, *U.S. Geol. Surv.*, 1–156.
- Wu, Y.-M., H. Kanamori, R. M. Allen, and E. Hauksson (2007). Determination of earthquake early warning parameters, τ_c and P_d , for southern California, *Geophys. J. Int.* **170**, no. 2, 711–717.
- Wurman, G., R. M. Allen, and P. Lombard (2007). Toward earthquake early warning in northern California, *J. Geophys. Res.* **112**, doi: [10.1029/2006JB004830](https://doi.org/10.1029/2006JB004830).
- Yeck, W. L., D. R. Shelly, K. Z. Materna, D. E. Goldberg, and P. S. Earle (2023). Dense geophysical observations reveal a triggered, concurrent multi-fault rupture at the Mendocino Triple Junction, *Commun. Earth Environ.* **4**, no. 1, 94.

Manuscript received 16 October 2023